



Norwegian University of
Science and Technology

Scale model measurements of headloss in unlined tunnels

Olukunle Benjamin Ekeade

Hydropower Development

Submission date: June 2017

Supervisor: Jochen Aberle, IBM

Norwegian University of Science and Technology
Department of Civil and Environmental Engineering

ABSTRACT

The purpose of this thesis work is to connect head loss coefficients in two different scale model tunnels to the physical roughness of the surface through measurements of head loss in fully turbulent flow and pressurized tunnel.

The thesis results shows that dynamic pressures measured at different position in the tunnel which was later converted to velocity reveals that the velocity decreases near the wall and the shape (parabolic) of the velocity profile suggests that the flow is turbulent and comparing hydraulic roughness coefficients calculated from Darcy-Weisbach and Colebrook-White equation led to agreement that hydraulic roughness in an unlined tunnel is some function of the height, spacing, density and nature of the physical roughness under consideration: the head loss depends on size of eddy generated which is directly proportional on the roughness projection that the eddy is spawned and the frequency of eddy generation is dependent on the spacing between consecutive roughness projections.

ACKNOWLEDGEMENTS

I would like to acknowledge and thank my supervisors Prof. Jochen Aberle and Dr. Pierre-Yves Henry for their support and guidance throughout this whole process, I am sincerely grateful for providing me with all the resources needed especially the financial assistance throughout my stay in Trondheim Norway to finish the thesis.

I am very thankful for the enthusiastic advice and laboratory assistance of Mr. Tesaker Geir and other technical staffs at the NTNU, hydropower laboratory and project mate Alvaro Gonzalez was kind enough to listen to my ideas and encouraged me.

Finally, I want to thank my family for all the support when I needed it the most and special thanks to my fiancé Olubukola Esther Akinola for her endless support and proofreading.

Table of Contents

ABSTRACT.....	i
ACKNOWLEDGEMENTS.....	ii
Table of Contents.....	iii
List of figures.....	v
List of tables.....	vi
Nomenclature.....	vii
CHAPTER ONE.....	1
1.0 INTRODUCTION.....	1
1.1 Background.....	3
1.2 Norway Hydropower Potential.....	3
1.3 History of Unlined Pressure Tunnels.....	4
1.5 Objectives.....	6
1.6 Thesis outline.....	6
1.7 Limitation of study.....	7
CHAPTER TWO.....	8
2.0 LITERATURE REVIEW.....	8
2.1 Design of unlined pressure tunnels.....	8
2.1.1 Rock mass quality.....	9
2.1.2 Hydrogeology.....	9
2.1.3 In-situ stresses.....	9
2.2 Unlined Tunnelling method.....	10
2.2.1 Drill and Blast.....	10
2.2.2 Tunnel Boring Machine (TBM).....	12
2.3 Estimation of losses.....	13
2.3.1 Frictional Losses.....	13
2.3.2 Singular Losses.....	15
2.3.3 Flow regime and fully developed flow.....	15
2.4 Methods to determine the hydraulic roughness of unlined tunnels.....	17
2.4.1 Rahm's Method.....	19
2.4.2 Colebrook's method.....	21
2.4.3 Priha's method.....	21
2.4.4 Reinius method.....	21

2.4.5	Huval’s method.....	22
2.4.6	Wright’s method	22
2.4.7	Johansen’s method.....	22
2.4.8	Solvik’s method	23
2.4.9	IBA method.....	24
2.5	Existing scale model tests of unlined tunnels	26
CHAPTER THREE		29
3.0	EXPERIMENTAL SETUP.....	29
3.1	Unlined tunnel model set up	29
3.1	Calibration of pressure sensor.....	31
3.2	Dynamic pressure.....	31
3.3	Pressure drop or Headloss.....	33
CHAPTER FOUR.....		34
4.0	RESULTS AND DISCUSSION	34
4.1	Calibration of Differential Pressure Sensor	34
4.2	Dynamic pressure.....	34
4.3	Velocity profile	36
4.4	Pressure Drop and Headloss	37
4.5	Comparison of roughness in both tunnels.....	39
CHAPTER FIVE		40
5.0	CONCLUSION.....	40
REFERENCES		41

List of figures

Figure 1: General layout of hydroelectric plants in Norway	5
Figure 2: Hydropower plant cross section with unlined waterways	9
Figure 3: Blasting profile for typical large tunnel	11
Figure 4: Typical tunnel view generated from a TLS point cloud.....	12
Figure 5: Velocity profile of turbulent flow	16
Figure 6: Moody's Diagram.....	17
Figure 7: show α and β calculation principle sketch.....	23
Figure 8: Principal sketch for calculating wall roughness	24
Figure 9: Principal sketch for calculating cross section roughness	25
Figure 10: Measuring procedures	29
Figure 11a: Tunnel A	30
Figure 11b: Tunnel B	30
Figure 12: schematic diagram of tunnel A & B showing cross-sections and strips spacing	30
Figure 13: schematic diagram of dynamic pressure measurement	32
Figure 14: schematic diagram of differential static pressure measurement.....	33
Figure 15: linearization of observed measurement against instrument measurement	34
Figure 16: dynamic pressure plotted against time for different charges.....	35
Figure 17: depicts the measured velocity as a function of position in the Tunnel.....	36
Figure 18: measured static differential pressure as a function of time (Tunnel B).....	37
Figure 19: measured static differential pressure as a function of time (Tunnel A)	38
Figure 20: Static pressure plotted against discharge.....	38

List of tables

Table 1: Hydropower capacity in Norway4

Table 2: The first unlined pressure shafts in Norway5

Table 3: Manning and Darcy-Weisbach roughness factor.....15

Table 4: Characteristics of the tunnels used in the study of Rahm.....20

Table 5: The head loss and friction factor for the experiment26

Table 6: Estimated Manning’s n values for concrete pipes27

Table 7: Average headloss, frictional factor and Relative roughness for Tunnel A.....39

Table 8: Average headloss, frictional factor and Relative roughness for Tunnel B39

Nomenclature

α_s = Head loss coefficient [-]

δ = Relative roughness [-]

ρ = Density [ML^{-3}]

A = Cross sectional area [L^2]

D = Diameter of circular channel [L]

D_m = Mean equivalent diameter [L]

D_n = Nominal equivalent diameter [L]

f = Frictional factor or Darcy-Weisbach frictional factor [-]

R_h = Hydraulic radius [L]

g = Acceleration due to gravity [LT^{-2}]

H = Total head or energy head [L]

h_σ = Standard deviation of roughness profile [L]

h_λ = Mean of roughness profile [L]

h_l = Head loss [L]

h_s = Head loss due to singular losses [L]

L_n = Total length of the tunnel stretch [L]

k = Hydraulic roughness [-]

k_s = Nikuradse's equivalent grain diameter [mm]

n = Manning's number [-]

Re = Reynolds number [-]

RMS = Root mean square

T = Number of points in the profile

P = Wetted perimeter of the channel [L]

p = Pressure [$ML^{-1}T^{-2}$]

v = Velocity [LT^{-1}]

Z = height above a datum [L]

CHAPTER ONE

1.0 INTRODUCTION

The world increasing usage of energy, have led to the high demand of energy, which requires adequate supply, environmental friendly and as well as sustainability to meet the future demand, it is in this framework, resources like water, fossil fuels, rare elements and wind energy and change in the global climate are important challenges for stakeholders in the energy sector. In recent years, the change of global climate and the associated increase of the mean annual surface temperature has become a major concern. It is evident that the major cause of global warming is linked to the burning of fossil fuels and the release of carbon dioxide and other greenhouse gases to the atmosphere produced in the process. The greenhouse effects of anthropogenic CO₂ emissions contribute 50 % of the observed global warming. There are many unwanted and on a long run very costly effects of global warming. The effects include displacement of vegetation zones, thawing of permafrost, melting of continental ice caps and associated sea level increase, melting of glacier ice in Alpine mountain ranges and associated effects on water and energy supply for large areas in mountain forelands, and predicted increase of extreme weather conditions. To tackle these important challenges, the change to focus on renewable and environmental friendly source of energy currently remains a vital role to stakeholders in energy sector. In the past few decades the use of fossil fuels and coal has increased the emission of greenhouse gases which has contributed to the effect of climate change, focus on thorough research in reducing the greenhouse gas emission and storage of the available energy have called on every individual from scientist to engineers, to economist and as well the public sectors must be involved in order to achieve a significant and sustainable achievement. Parallel to the development of “renewable” energy, energy must be used more efficient, conversion losses must be reduced, energy saving must be made attractive. Energy efficiency requires new inventive technologies. Water is one of our most vital resources in our environment.

One of the vital uses of water in the world is using it as a source of energy. Hydropower, simple concept of this type source of energy is that, force of water flowing through a dam rapidly turns the rotary blades (usually made of metal) that are attached to the generators thereby producing electricity. There are three types of hydropower stations: (i) run-of- river, which the principle is simply that energy is generated through flowing of a river (ii) reservoir type, electricity is produced

the release of water storage (iii) pump storage, water stored is being pumped back in a higher stored facilities in order to be released again. The advantages part of hydropower is: (a) fuel is not used making it one of the ways in reducing greenhouse gas emissions (b) water used in the power plant is mostly as a result of nature (c) the technology proven over time is reliable and sustainable (d) most important is renewable. Due to all these advantages makes hydropower source of energy a very great degree factor, since the maintaining the emission of greenhouse gases is one of the greatest environmental challenges facing the world today. In addition to its advantages contributions in combating resources depletion and global warming, hydropower plays an important role in river systems; while river system regulations provides protection for people and environment from floods and drought in wet and dry season respectively.

Hydropower supplies 71% of all renewable source of energy, reaching 1064GW of installed capacity in 2016, it generated 16.4% of the world's electricity from all energy sources (WER, 2016). Harnessing water responsibly can help get electricity to millions of people, especially in sub-Saharan Africa and South Asia where lack of access to power is most acute. Many hydropower plants in the world profit from various storage systematic plans and in several river schemes, certain amount of power stations are station outpouring one after the other, in order that the water can be utilized so many times before it finally flows out in the river or sea. In speeding the economic growth in Europe and North America during the twentieth century, hydropower in these regions was extensively developed and progress has continued until present day. A number of the world's most electricity-poor countries also have some of the least exploited hydropower potential, and hydropower represents the most economically viable, large scale source of energy for their development – particularly in Sub Saharan Africa. (George, 2016)

A very good importance of hydropower tunnels is the use to convey water up to the turbine driving the generators, then allowing it to discharge water into the river downstream. One of the major constituting parts of a water conveyance system is water conducting system, which is of two types; open channel flow system and pressure flow system (closed conduit type), hydropower tunnels may either be unlined (in case of quite good quality rocks) or lined with concrete or shot-crete. Most of the hydropower water tunnels are usually excavated by method of tunnel boring method (TBM) or the drill and blast method. Both methods used in excavation of tunnels have a great effect on the roughness of the tunnel, also geological conditions and geology plays a role. Drill and blast method

is a fast method of constructing tunnels in comparison with tunnel boring method; it simply involves the use of explosives and generally results in higher but lesser duration of vibration levels.

1.1 Background

Incomplete technical data and literature on the wall roughness of unlined tunnel, which left after excavation has led to the development of an improved methodology of estimating the head loss coefficient along the tunnel and thus to a more accurate prediction (Hákonardóttir *et al.*, 2009). In recent years, the use of laser scan technology in hydropower is becoming used in a rapidly increasing rate and becoming the quickest, safest and accurate approach to document valuable information like roughness of the tunnel wall which is associated to friction of the tunnel and therefore used to derive a meaningful approaches for the estimation of hydropower tunnel discharge capacity.

The data collected from laser scan can be used as input measurement for physical scale model in constructing up miniature version of the tunnel. Importance of such scale model of tunnels is to relate the experimental result of frictional and energy losses to the physical structure of tunnel roughness. The ability to have scale model is very beneficial because it has the detail necessary to make it realistic and understand more about the concept and to predict future losses. In recent years, most experimental setup of such scale model with unlined tunnel consists of a closed loop water system with non-circular Glass Acrylic (Perspex) or Plexiglas channel and replicating the rough tunnel surface with strip-roughness, such strip-roughness was designed at Norwegian University of Science and Technology (NTNU) and proved of generating different flow model therefore, serve as hydraulic resistance in a real rock blasted-tunnel.

1.2 Norway Hydropower Potential

It is important to point out Norway is the sixth largest hydroelectric power producer in the world; Norway has been a major producer of hydroelectric power for more than a century. The country possesses natural resources and a geography that enables to build environment-friendly hydroelectric stations For example European Union has installed 24.4% hydropower capacity making European Union second region exploiting this source of energy and more than 50% of the total situated in Norway, recently Norway have established hydropower capacity amount 30,000(MW) and annual production averages 125TWh (Norwegian Ministry of Petroleum and Energy 2008).

Power station	County	Max. capacity(MW)	Mean ann. Production (GWh)
Kvilldal	Rogaland	1240	3517
Sima	Hordaland	1120	3441
Tonstad	Vest-Agder	960	4169
Aurland	Sogn og Fjordane	840	2419
Saurdal	Rogaland	640	1300
Rana	Nordland	500	2123
Tokke	Telemark	430	2221
Tyin	Sogn og Fjordane	374	1398
Svartisen	Nordland	350	1996
Brøkke	Aust-Agder	330	1407
Evanger	Hordaland	330	1380
Nedre Vinstra	Oppland	308	1206
Skjomen	Nordland	300	1164
Vinje	Telemark	300	1003
Kobbelv	Nordland	300	733
Aura	Moere og Romsdal	290	1774

Table 1: Hydropower capacity in Norway

Table 1 shows the largest hydropower stations in Norway in 2008; Kvilldal, Sima and Tonstad being the most important ones with an average annual production of 3,517 Gigawatt hours (GWh), 3,441 GWh, and 4,196 GWh, respectively. Hydropower currently constitutes about 96% of the Norwegian electricity production compared to the 11% in the European Union. In this regard, Norway has obtained more knowledge covering all aspect of hydropower development, from planning and design to the delivery and installing of technical equipment. More importantly, there are always been strong focus on achieving environment-friendly practices, one of the Norwegian hydropower experience is the development of underground powerhouses, according to Broch (2013), presently about 200 powerhouses are located in Norway, as of recent 4000km of tunnels has been excavated. Estimations by Norwegian Ministry of Petroleum and Energy (2008) indicate that the available hydropower potential in the country is about 205TWh, out of which around 45.5TWh are located in protected areas. 121.8TWh has already been developed, leading to a remaining potential for development of 37.7TWh.

1.3 History of Unlined Pressure Tunnels

The Norwegian hydropower sector has over more than 100 years knowledge and skills in the design and construction of underground works, the implementation of unlined pressure tunnels in Norway hydropower constructions dated as early as 1919, emphasis was given to keep all waterway system and powerhouses inside the mountain mainly after the completion of World War II, due to shortage

of steel leading to uncertain delivery and very high prices. One such of the country specialty is the unlined, high-pressure tunnels and shafts. Unlined in this context means a water tunnel without steel lining or hydraulic concrete lining, with rock support only consisting of rock bolts alone or in combination with sprayed concrete applied only on parts of the tunnel surface, thicker reinforced sprayed concrete or shorter concrete sections where required (Broch, 1982B, 2000).

Name	Year	Water head (m)	Diameter (m)	Experience
Herlandsfoss	1919	136	3.20	Partly failed
Skar	1920	129		Completely failed
Svelgen	1921	152	2.40	Minor leakage
Toklev	1921	72	2.50	No leakage

Table 2: The first unlined pressure shafts in Norway

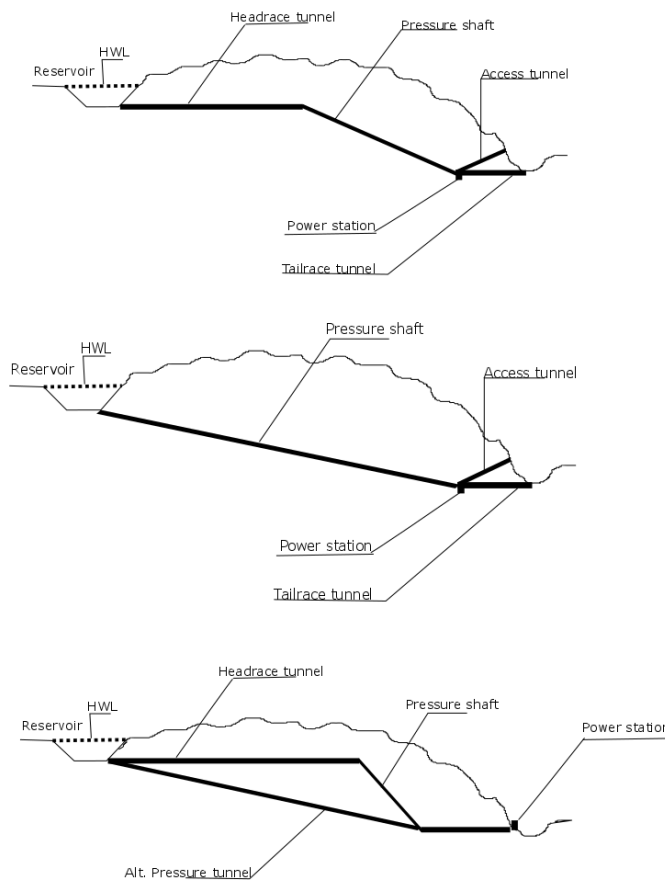


Figure 1: General layout of hydroelectric plants in Norway

The typical design of the hydropower plants before 1940s include horizontal headrace tunnel, penstock along the surface topography and powerhouse on the bottom of the valley (Palmstrøm, 1988). Certainly, there had been attempts in the early 1920s to build underground pressure shafts (both steel lined and unlined) and underground powerhouse (Panthi and Basnet, 2016). The first such hydropower scheme with underground powerhouse was built in the year 1919. Four hydropower schemes were built during this period, they were designed with low pressure headrace tunnel, unlined pressure shafts and include horizontal penstock tunnel as water conveyance system connecting the powerhouse which situated at the surface. Three of these projects had problems of complete failure or leakages (Table 2) but were later solved by introducing grouting and extension of penstock pipe. Reducing steel lined sections and utilizing unlined tunnel sections are important to achieving an economical project.

1.5 Objectives

To investigate the different methods in constructing Hydropower tunnels

To investigate different methods of determining the roughness of Hydropower tunnels

To measured physical roughness in tunnels to hydraulic roughness

To cross-check and validate the methodology of strip-roughness designed at NTNU through model tests in the NTNU hydraulic laboratory within the framework of the research project Tunnel-roughness

1.6 Thesis outline

Chapter one: In this chapter the introduction to the study; reason and importance of renewable energy is discussed, the urbanization and increase in world population have led to more energy demand, it has been linked that use of fossil fuels contribute to climate change, however tackling this problem the need to focus on renewable and environmental friendly source of energy currently remains a vital role to stakeholders in energy sector. Hydropower has a lot of advantages from fuel is not used making it one of the ways in reducing greenhouse gas emissions to the fact that is renewable. Hydropower supplies 71% of all renewable source of energy, reaching 1064GW of installed capacity in 2016, it generated 16.4% of the world's electricity from all energy sources. Scale model of tunnels is important and proven very beneficial because it has the detail necessary to make it realistic and understand more about the concept and to estimate future losses relate the experimental result of frictional and energy losses to the physical structure of tunnel roughness.

Chapter two: The literature review of methods used in construction of unlined tunnel and theoretical foundation of estimating losses is highlighted; During tunnel excavation, wall roughness is created due to the variation in section geometry which affects the friction factor and therefore also affects the frictional head losses in the tunnel; the difficult situation of measuring hydraulic losses in waterway tunnel is of highest degree significance to engineers involved in hydropower development. Head losses in unlined tunnels are controlled by many factors e.g geology properties of the rock, method of excavation, the size and diameter of the tunnel is possible easily measure these losses in monetary terms, because hydraulic head consequently leads to a reduction revenue, it is essential to estimate head losses in the tunnel not only in the design stage but also in the planning so that the effect can be added to the whole engineering and economic analysis of the project. Several authors have proposed methods of estimating frictional losses in lined and unlined tunnel based on method of excavation.

Chapter three: In this chapter, the experimental setup of the model was discussed, emphasis will be placed on how the roughness of both tunnels is created, the dimension of the tunnel and as well as the measuring campaign procedures is explained.

Chapter four: The results and discussion of the measurements and calculations described in the third chapter are presented and discussed. Comparisons between results are made where these are relevant.

Chapter five: The conclusion of the study is discussed.

1.7 Limitation of study

This study was supposed to be a scale model of a physical model of an unlined tunnel in Norway, however, it was not possible to work on the actual scale model which was in the thesis plan due to construction constraints. All measurements and readings in this thesis work were carried out on two existing scale models at Norwegian University of Science and Technology, hydropower laboratory, Trondheim, Norway.

CHAPTER TWO

2.0 LITERATURE REVIEW

Construction of hydropower plants involves a substantial utilization of tunnels and underground caverns, methods use in the design and construction of tunnels and underground caverns have contributed to the tunneling concepts. Before any kind of underground project could be done, pre-construction investigations of high quality and well adapted to the geological conditions and the project characteristics are crucial. If the analysis is inadequate or lack the quality of design, unforeseen and sometimes irresistible ground condition could be encountered which always lead to poor quality and excess cost of the project.

Pre-construction investigation, often simply called pre-investigation, thus is very important for evaluating the feasibility of the project and for planning and design (Nilsen & Palmstrøm, 2000). The principal objective of pre-investigation is to apply best methods of constructing tunnels for specific geological conditions and that aim at making the tunnel suitable enough for its purpose. Carrying out pre-investigation is to supply adequate information in order to design and consider the consequences of constructing the tunnel. Fischer *et al.* (2009), stated that the focus should be on providing enough information to develop reliable predictions of ground conditions and ground behavior during construction. Good method of pre-investigations and good site investigation methods will be advantage all stakeholders participating in before and after decision of constructing unlined tunnels. During pre-investigations for rock engineering, permeability tests of different kinds are performed in order to characterize the hydraulic properties of the rock. Appropriate and well carried out pre-constructions extend the understanding of the ground, hence lower the probability for abrupt problems, however it is important to point out that ground investigations expose all ground formation therefore it is always possible to encounter unforeseen conditions.

2.1 Design of unlined pressure tunnels

Some special techniques and design concepts have over the years been developed by the hydropower industry. In constructing unlined pressured tunnels, rock quality must be able to resist the internal water pressure in terms of both leakages and deformation which can subsequently cause failures, the rock mass must be such that it has low permeability, rock mass with high permeability will possibly lead to water seeping into and out of the tunnel depending on the connectivity of the groundwater

movement and the pressure in the tunnel. Some other factors affecting the design of unlined pressure hydropower tunnels are discussed below.

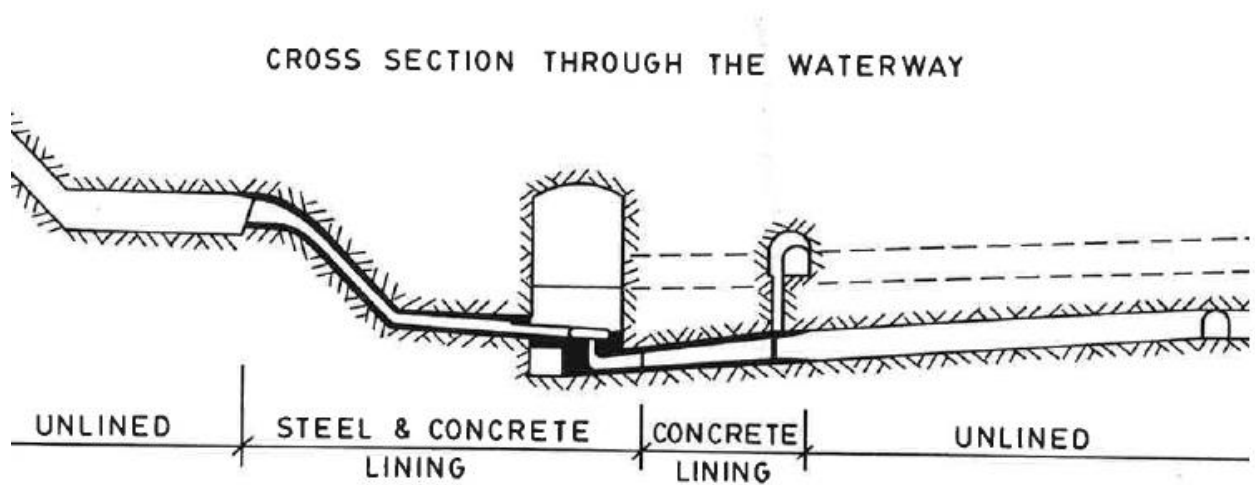


Figure 2: Hydropower plant cross section with unlined waterways. (Broch, 1984)

2.1.1 Rock mass quality

The primary criterion that must be met by an unlined pressure tunnel is that the hydrostatic head must be less than the minimum principal stress in the rock mass surrounding the tunnel at all points. Where this criterion cannot be satisfied, a steel liner must be used to isolate the pressurized tunnel water from the surrounding rock. However, because of its intrinsic complexity, it requires considerable attention in order to characterize heterogeneity, anisotropy, and non-linearity and identify associated uncertainties (Hudson et al., 2001).

2.1.2 Hydrogeology

This section addresses the natural pore pressure distribution around the tunnel and thus, the effective hydraulic pressure driving in or out of the tunnel. This pressure results from the action of the internal tunnel pressure together with the natural rock mass pore pressure that was initially acting along the tunnel vicinity. In evaluating the amount of water flowing in or out of the tunnel, a high initial (natural) pore pressure will limit the total amount of flow out of the tunnel (Deere, 1983).

2.1.3 In-situ stresses

The minimum principal stress is the basis of the Norwegian approach, which stated that if the minimum stress is smaller than the water pressure around a tunnel, any existing joints perpendicular to the minimum stress will tend to open, thus creating hydraulic jacking conditions (Broch, 1982).

Pressure tunnels are often constructed near the ground surface where there are open and weathered joints, and where more decompressed rock masses are encountered. For any project, the in-situ stress must be first estimated at the preliminary stage, and later measured from the surface at the exploration and design stage.

2.2 Unlined Tunnelling method

Predominantly construction of unlined tunnels is carried out by excavation, the choice of construction method is acutely influence by the geology, project specific conditions such as tunnel length and cross section and also depends on the cost of the project. Tunnel construction are defined a number of different factors. Tunnel excavation can be seen as a cyclic process with the main activities executed in series, one of these is the way the construction process is executed. According to Salazar (1985) and Müller (1978) the tunnel construction process can be described as a “series” system, where the main activities lie in series along the critical time path. There are three main method of tunnel excavation: Drill and Blast, Tunnel Boring Machine (TBM) and Road header. Subchapters below will described how they are applied, basic operations, how they are carried in different situation.

2.2.1 Drill and Blast

Drilled and blasted tunnels are excavated in a cyclic process, beginning with the use of a drilling machine to make holes into the rock surface cycle (Tarkoy, 1995). With the discovery of the explosives, this is more efficient and powerful than gun powder, the invention made explosives possible in tunnel construction. At the same time the invention of more powerful steam and air compressed drills made the development of the drill and blast tunneling method possible. The concept of this type of tunneling is that drilling machine drill holes where the explosives are fixed to the wall of the rock. In most cases the holes are parallel into the rock face but it is also possible to create fan shaped cuts, where the holes are drilled in at an angle. Bruland & Sohkrallah, (2001) reported that fan shaped drilling is more effective than parallel because it creates a larger free face in each explosion. It is, however, harder to drill correctly and therefore not used as much today.

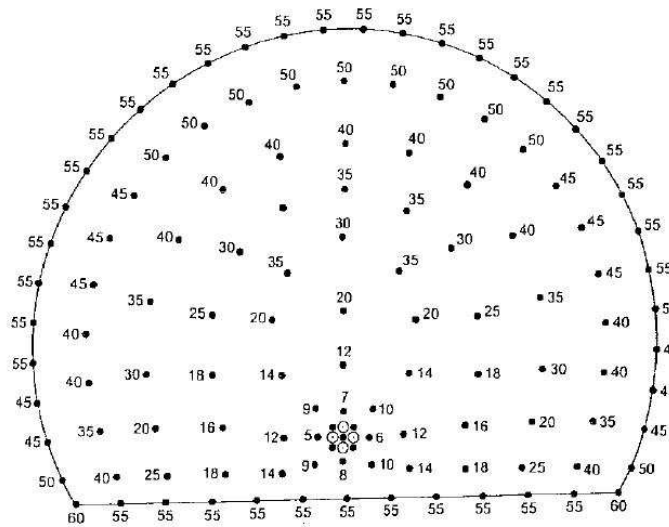


Figure 3: Blasting profile for typical large tunnel (Arngrímsson & Gunnarsson 2009)

The level of automation and mechanization of these tasks is low and there is a high degree of hard manual labor involved. After the holes are drilled they are filled with explosives, large hole created at the middle of the rock surface is left without explosives which serve as a free face. A free face is created so that the explosives can blast the rock into the space. If there is no free face the rock will only crack and is still left relatively intact (Arngrímsson & Gunnarsson 2009). When the explosives have been connected, they are blown in a certain orderliness to ascertain that each circle of charges is blown into the left spaces by the preceding charges, conventionally starting in the middle; the blown region is ventilated so that toxic gasses and dust (muck) is not left in the vicinity. Loose materials are removed and the rock support is attached as required, example of such rock support can be rock-bolts, shot-crete lining or cast in place concrete lining is as a rule used only for stability purposes. In some cases the process of the support phase is left for a few drill and blast cycles and then done all at the same time. According to Eydísardóttir (2013) for drill and blast tunnels the roughness depends mainly on four different factors. One of them is the change in cross section of the tunnel. For drill and blast tunnels the cross section will not be constant throughout the length of the tunnel. The roughness also depends on the roughness of the tunnel invert, the wall roughness and the material roughness. The effect of material roughness on the total roughness has not been thoroughly investigated and it is therefore not clear how large this is contribution to the tunnel roughness (Rønn, 1997).

The drill and blast excavation method is a very adaptable and flexible process in regard to the excavation of any tunnel cross section or intermediate section, and it allows for the installation of various kinds of temporary rock support. Further, the drill and blast method is characterized by a short mobilization time requirement due to the use of standard equipment. The degree of roughness in drill and blast tunnels is higher than that of TBM tunnels.

2.2.2 Tunnel Boring Machine (TBM)

This method of excavation involves the use of Tunnel Boring Machine. A tunnel boring machine (TBM) typically consists of one or two shields (large metal cylinders) and trailing support mechanisms. At the front end of the shield is a rotating cutting wheel, behind the cutting wheel is a chamber. The chamber may be under pressure (closed machine) or open to the external pressure (open machine), below the chamber there is a set of hydraulic jacks supported by the finished part of the tunnel which push the TBM forward. The rear section of the TBM is braced against the tunnel walls and used to push the TBM head forward.



Figure 4: Typical tunnel view generated from a TLS point cloud. (Aberle, *et al.*, 2017)

At maximum extension the TBM head is then braced against the tunnel walls and the TBM rear is dragged forward back of the shield, inside the finished part of the tunnel, several support mechanisms which are part of the TBM are located: soil/rock removal, slurry pipelines if applicable, control rooms, and rails for transport of the precast segments. Braitveit (2015) reported that head loss of an unlined tunnel excavated by drill and blast is 3-4 times greater than that of a bore tunnel of the same cross sectional area, due to the rough surface and larger cross sectional variation.

2.3 Estimation of losses

Like other type of water conveyance systems, cross sections and shapes of an unlined TBM, drill and blast tunnel vary randomly from one section to another, for drill and blast tunnels horse-shoe cross section are usually adopted while TBM tunnels are normally circular cross section after excavation, due to irregular projections on the wall surface during excavation causes micro-roughness to be generated which then lead to continuous expansion of roughness, hence offers high resistance to flow (As shown on figure 4). The flow in the tunnel lacks longitudinal and lateral symmetry (Aberle, *et al.*, 2017).

Subsequent sections briefly describe hydraulic head losses in tunnels.

2.3.1 Frictional Losses

Flow in water conveyance systems are based on the universal principles of fluid flow. When a viscous fluid (real) flows through a tunnel or pipe part of its energy is dissipated in sustaining the flow. Total energy of the flow is given as:

$$H = \frac{v^2}{2g} + \frac{p}{\rho g} + z \quad (2.1)$$

As a result of the internal friction and turbulence, the total energy is no longer constant along the medium, due to the friction along the direction of flow leads to the expression of the energy loss in terms of the fluid height termed as the head loss and usually classified into two categories, the first type is called the frictional losses or major losses.

$$\frac{v_1^2}{2g} + \frac{p_1}{\rho g} + z_1 = \frac{v_2^2}{2g} + \frac{p_2}{\rho g} + z_2 + \Delta h_l \quad (2.2)$$

$$\Delta h_l = \frac{p_1 - p_2}{\rho g} \quad (2.3)$$

In the last decades, more studies have been carried out, in order to investigate and formulate precise relation of the diverse types of head losses mostly in rough and smooth pipes, recently less studies have been carried out on unlined tunnels. Weisbach (1855) was the first person to carry out a relation for head loss. According to Lahiouel & Lahiouel (2015), Darcy contributed greatly to the application of the derived relation, thus associating his name with that of Weisbach. The relation is therefore most commonly known as the Darcy-Weisbach formula, it relates the head loss, frictional factor,

length of the channel and diameter of the channel. Darcy-Weisbach equation (Equation 2.4) shows that as head losses increases so as roughness increases and decrease with increased diameter. The friction coefficient, the flow velocity and the pipe dimensions:

$$h_l = f \frac{L*V^2}{D*2g} \quad (2.4)$$

Elger et al., (2012) and White, (2009) accounted that Darcy-Weisbach is not only used for circular pipes but also for non-circular section, in this case the hydraulic diameter is used instead of the diameter. The hydraulic diameter is calculated with Equation (2.5).

$$D = R_h = \frac{4A}{P} \quad (2.5)$$

Bishwarkarma (2012) reported that Darcy-Weisbach and Manning's formulae give approximately the same result when the relative roughness value is between 25 and 2000. Manning's formula, which is an empirical equation, is also widely used in calculating major losses in a tunnel.

$$h_l = f \frac{LV^2 n^2}{R_h^{1.33}} \quad (2.6)$$

In many countries Manning's formula (Equation 2.6) is still widely used in calculating head loss in tunnels, nevertheless, it should be noted there are some limitations in using Manning's formula. One of these limitations was reported by Solvic (1988) that if using absolute roughness, the head loss calculation will be wrong outside the roughness range when using Manning's formula. The Manning's Formula is developed for open channel flow and subsequently adapted for pipe flow, is generally applicable for conduits with diameters greater 2m, whereas the Darcy-Weisbach formula is theoretically suitable for a wider range of roughness values (Benson, 1989).

Lining	Manning's "n"	Comparable Darcy-Weisbach "f" for varying diameters			
		2.5m	5m	7.5m	10m
Unlined (D&B)	0.025-0.040	0.057-0.147	0.046-0.117	0.040-0.102	0.036-0.093
Unlined (TBM)	0.016-0.022	0.023-0.044	0.019-0.035	0.016-0.031	0.015-0.028
Shotcrete (D&B)	0.018-0.025	0.030-0.057	0.024-0.046	0.021-0.040	0.049-0.036
Concrete	0.012-0.016	0.013-0.023	0.010-0.019	0.0092-0.016	0.0083-0.015
Steel	0.010-0.014	0.0092-0.018	0.0073-0.014	0.0064-0.012	0.0058-0.011

Table 3: Manning and Darcy-Weisbach Roughness factor (Benson, 1989)

2.3.2 Singular Losses

The second category of losses is called singular or minor losses, In addition to the above described major frictional losses, tunnels are also subjected to minor or singular losses due to the change in alignment, lining, over-breaks and construction facilities such as niches. In addition to the above described major frictional losses, tunnels are also subjected to minor or singular losses due to the change in alignment, lining, over-breaks and construction facilities such as niches (Bishwarkarma 2012). The most common method used to determine these head losses or pressure drops, Bratveit et.al, (2015) used this method to describe the sum of the head losses due to minor rock fall in unlined tunnel as;

$$\Delta h = \sum_{i=1}^s h_s = k_s \frac{v^2}{2g} \quad (2.7)$$

Most values of k are found by experiment, careful judgment is required to ensure that Reynolds number values in the application correspond to the Reynolds number values used to acquire the data (Elger et al., 2012).

2.3.3 Flow regime and fully developed flow

The friction coefficient is a function of the flow regime characterized by the Reynolds number. Flow in a pressurized tunnel is classified as being laminar, transitional or turbulent depending on the magnitude on the magnitude of the Reynolds number. If the fluid velocity in a pipe is small streamlines will be straight, as the velocity steadily increases, streamlines remains straight and

parallel with the pipe until velocity is attained such that the streamlines breaks in a diffused patterns, at this point the velocity is “critical”.

$Re \leq 2300$	<i>Laminar flow</i>
$2300 \leq Re \leq 4000$	<i>Transitional flow</i>
$Re \geq 4000$	<i>Turbulent flow</i>

In laminar flow, the velocity is lower than the critical velocity, laminar regime of flow the velocity is highest on the pipe axis, and on the wall the velocity is equal to zero while when the velocity is greater than critical velocity, the regime of flow is turbulent. In the turbulent regime of flow, there is always a thin layer of fluid at pipe wall which is moving in laminar flow. That layer is known as the boundary layer or laminar sub-layer. It turns out that the transition from laminar to turbulent flow also depends on the degree of disturbance of the flow by surface roughness, pipe vibrations and fluctuations in the flow (Elger *et al.*, 2012; White, 2010).

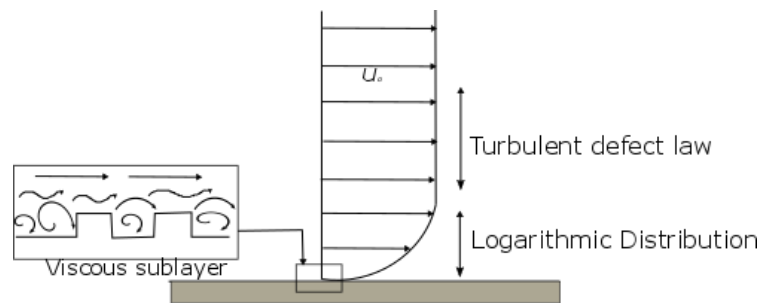


Figure 5: Velocity profile of turbulent flow

As fluid enters a pipe or channel, boundary layers keep increasing until they meet after some distance downstream from the entrance region. After this distance velocity profile doesn't change, flow is said to be Fully Developed. Powe and Townes (1973) investigated the turbulence structure for fully developed flow in rough pipes. The method used to determine the turbulence structure involved examination of the fluctuating velocity spectra in all three coordinate directions. An important conclusion of this work was that in the central region of the pipe, the flow was relatively independent of the nature of the solid boundary. In contrast, the flow near the wall presents a marked dependence on the nature of the solid boundary.

Several authors have shown different ways of representing the effects of rough surfaces on turbulent flows. Webb *et al.* (1971), in their experimental study of tubes with rough walls, developed a friction factor correlation based on the law of the wall similarity. In more recent work, Koh (1992) presented an equation to represent the mean velocity distribution across the inner layer of a turbulent boundary layer, and used this velocity profile to derive a friction factor correlation for fully developed turbulent pipe flow.

2.4 Methods to determine the hydraulic roughness of unlined tunnels

Various explicit and implicit relationships were proposed for the friction coefficient f or hydraulic roughness k . Nikuradse (1933) carried out substantial investigation which involves the effect of wall roughness with respect to pressure decline and discharge in a pressurized flow conduit, also in this report the relationship between Darcy-Weisbach friction factor to wall roughness and dimensionless Reynolds was obtained.

When the friction factor is calculated, traditionally the tunnel roughness is described by Nikuradse's equivalent sand-grain roughness, also called hydraulic roughness. To be able to calculate the friction factor the physical roughness of the tunnel needs to be converted to Nikuradse's equivalent sand-grain roughness i.e. hydraulic roughness. The friction factor is then used to calculate the frictional head loss (Eydísardóttir, 2013).

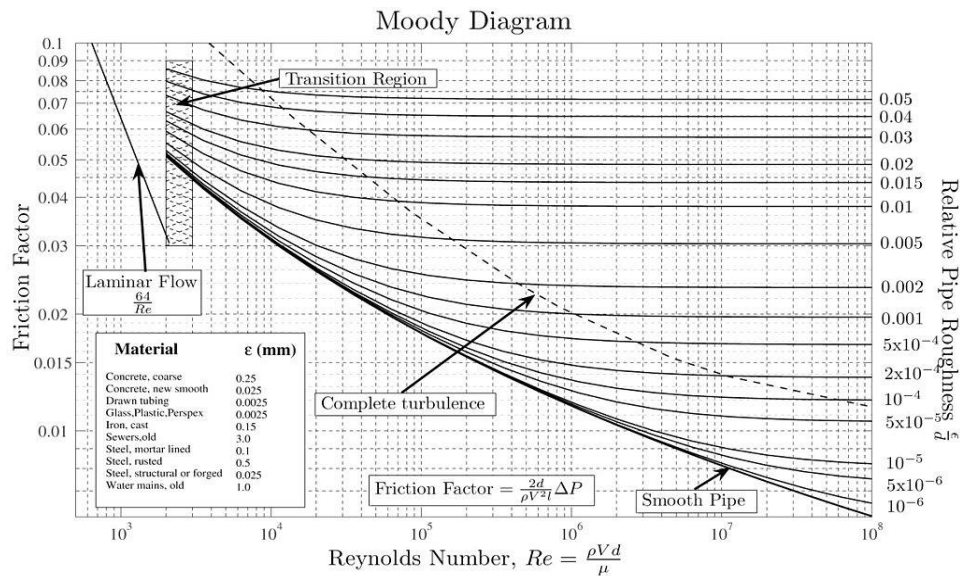


Figure 6: Moody's Diagram (White, 2009)

Colebrook (1939) proceeded with Nikuradse's work by acquiring data for commercial pipes and then developed an empirical equation, called the Colebrook-White formula (Equation 2.8a), for the friction factor related to a given Reynolds number. Transition zone of the rough regime of the Colebrook-White formula shows monotonic changes the skin friction which is becoming increasingly exact as a variable approaches hydraulically smooth condition at low Reynolds number and the fully rough state at high Reynolds number.

$$\frac{1}{\sqrt{f}} = -2 \log_{10} \left(\frac{k_s}{3.71D_h} + \frac{2.51}{Re\sqrt{f}} \right) \quad (2.8a)$$

Moody (1944) developed a design chart by using Colebrook-White formula (Equation 2.8) universally known as Moody's Diagram (Figure 6), the chart allows the determination of the friction coefficient as a function of the Reynolds number and the ratio (k_s/D). The frictional factor curves on the Moody's diagram are based on f in the equation (2.8a) tested for of commercial pipes (galvanized iron, wrought iron, and tar-coated cast iron). While the Moody diagram has been and will continue to be an incredibly useful engineering tool for estimating the pressure losses in pipe flow, it has some significant practical limitations. Moody understood some of these issues and stated that he expected the friction factor obtained from the diagram to be accurate within about 10%. Flack & Schultz (2014) highlighted some limitations of the Moody diagram First, it is only strictly valid for surfaces in which the equivalent sand roughness height (k_s)(ϵ as shown on the diagram) is known apriori and that are operating in the fully rough regime. With regards to the first condition, k_s is not a physical measure of the surface roughness but is instead the uniform sand roughness height from Nikuradse's experiments that produces the same friction factor as the surface of interest in the fully rough regime. Because of this, a hydrodynamic test in the fully rough regime is required to determine k for a generic roughness before its skin-friction can be predicted. Numerous researchers since the last decades have performed additional tests for a range of rough surfaces as listed on the Moody diagram. Changes in surface geometry originating from wide ranges of factor such as excavation method, surface preparation, coating application and as well as the fouling of the surface can greatly change the equivalent sand roughness height for a surface. Hydraulic roughness is generally regarded as a function of height; spacing, density and shape of the physical roughness for a given flow type (Hákonardóttir *et al.*, 2011).

For hydraulically rough or fully developed flow at high Reynolds numbers which is usually encountered in tunnels equation (2.8a) is reduced to:

$$\frac{1}{\sqrt{f}} = -2 \log_{10} \left(\frac{k_s}{3.71 D_h} \right) \quad (2.8b)$$

A kind of equivalent approximation of equation (2.8b) in estimating the Darcy-Weisbach frictional factor directly using standard deviation of a roughness profile σ by Heerman (1968) equation:

$$\frac{1}{\sqrt{f}} = 4.3 \log_{10} \left(\frac{D_h}{\sigma^{1.66}} \right) - 3.71 \quad (2.8c)$$

Equation (2.8c) was obtained by coupling measured mean velocity in a turbulent pipe flow to a presumably derived shear velocity; the aim of the study is check how relevance is the spacing between specific roughness elements by repeatedly modifying wave length of the pipe interior roughness. Many researcher have developed

2.4.1 Rahm's Method

Rahm (1958) conducted a study on linear head loss in rock tunnels in Sweden, choosing thirteen tunnels under pressure. Table 4 shows some characteristics of these tunnels that are part of hydraulic circuits of hydroelectric plants. Through this investigation, Rahm (1958) found a relation that shows that the head loss is proportional to relative roughness; the frictional factor f is independent of Reynolds number (Re) and is dependent on the roughness in the tunnel cross-sectional area. The method requires the discretization of the areas along the tunnel (suggesting approximately 5m distance between measurements). A statistical distribution of the normal type from which certain areas of the cross-section are determined with 99% and 1% of cumulative frequency is applied over the measured area values.

The determination of a relative roughness δ is done by Equation (2.9):

$$\delta = \frac{A_{99\%} - A_{1\%}}{A_{1\%}} * 100\% \quad (2.9)$$

Tunnel	Length (m)	Area (m²)	D_h (m)	Rock types	f
Alfta (A)	3025	33.8	6.16	Granite-gneiss	0.086
Blåsjön (B)	5620	57.1	8.16	Gneiss-mica-shale	0.047
Dönje (D)	4700	141,3	12.84	Gneiss	0.7
Harsprånget (H)	2430	204.0	15.4	Granite	0.052
Järpströmmen (J)	4520	114.3	11.52	Silurian slate	0.048
Krokströmmen (K)	2196	101.6	10.88	Granite	0.048
Nissaström (N)	1465	36.6	6.52	Granite-gneiss	0.101
Porjus I (PI)	1194	57.4	8.63	Granite-gneiss	0.073
Porjus II (PII)	1032	61.5	8.64	Granite-gneiss	0.055
Selsfors (Se)	629	80.5	9.68	Black slate with granite intrusion	0.114
Sillre (Si)	1829	6.6	2.84	gneiss	0.102
Sunnerstaholm (Su)	330	35.9	6.48	Granite-gneiss	0.104
Tåsan (T)	6698	17.2	4.48	gneiss	0.081

Table 4 - Characteristics of the tunnels used in the study of Rahm (1958)

The relation between this relative roughness δ and the absolute equivalent roughness k can be represented by Equation (2.10):

$$\delta^{-0.5} = 0.105 * \log \frac{15R_h}{k} \quad (2.10)$$

The relationship between frictional factor and relative roughness is given as:

$$f = 2.75 * 10^{-3} * \delta \quad (2.11)$$

2.4.2 Colebrook's method

Colebrook (1958) stated the Colebrook's method for estimating frictional factor, in this method the overbreak tm of an unlined tunnel is defined as half the difference between the mean hydraulic diameter and the hydraulic diameter of the area with 1% cumulative frequency of occurrence. tm is equal to the absolute roughness k of the surface. The value of the linear friction coefficient is calculated by Equation (2.12)

$$f = 0.55 \frac{R_h^{1.5} * t_m}{(R_h^{1.5} + t_m)^{2.5}} \quad (2.12)$$

2.4.3 Priha's method

Priha (1969), further worked on Rahm's (1958) idea but limit the studies to small ($6m^2$) unlined rock tunnels. A large number of tunnels were tested and an additional relationship was found that better suited small tunnels. From the investigation the study proposed the following relationship:

$$f = 3.31 * 10^{-3} * \delta * \left(\frac{A_{1\%} + 9}{A_{1\%}} \right)^{0.5} \quad (2.13)$$

2.4.4 Reinius method

In the study, an empirical relationship between the friction factor and the relative over-break of the tunnel was developed. The method proposed that if tunnel is constructed in the direction of flow, there would be more head losses than if the construction is in opposite direction, depending on the type of execution and considering the relative roughness (δ). Also proposed range of values, giving equations for a mean, minimum, and maximum value based on the type of excavation technique, minimum for smooth blasting and a maximum value for rapid blasting. Reinius (1970) derived different friction coefficients are empirically given for normal, slow and rapid progress of work.

Normal excavation the friction factor f is described by

$$f = 0.02 + 0.0016 \times \delta \quad (2.14a)$$

Careful excavation the friction factor is

$$f = 0.03 + 0.00085 \times \delta \quad (2.14b)$$

And, for a rapid excavation, the friction factor is

$$f = 0.01 + 0.0027 \times \delta \quad (2.14c)$$

2.4.5 Huval's method

Huval (1969) presents a method for computing an equivalent roughness for unlined rock tunnels that is employed for different tunnel stretches. Roughness is measured as the difference between the mean equivalent diameter (D_m) and the nominal equivalent diameter (D_n) of the tunnel cross section. This roughness is equal to the equivalent hydraulic roughness k .

$$k = D_m - D_n = \sqrt{\frac{4}{\pi}} (\sqrt{A_m} - \sqrt{A_n}) \quad (2.15)$$

2.4.6 Wright's method

The method considers natural overbreak t_n of an excavated tunnel according to equation (2.16)

$$t_n = \frac{A_{50\%} - A_{1\%}}{0.5(P_{50\%} + P_{1\%})} \quad (2.16a)$$

The relative overbreak is calculated from equation (2.16b)

$$\delta = 2 * \frac{t_n}{R_{50\%}} \frac{1}{\left(1 - \frac{t_n}{2 * R_{50\%}}\right)^2} * 100\% \quad (2.16b)$$

When the value of relative overbreak δ , the author produced a graph where friction coefficients are related to relative overbreak for an exposed drill & blast rock tunnel or with a concrete lined invert of a drill & blast unlined tunnel.

2.4.7 Johansen's method

The absolute roughness for a cross section can be estimated in equation (2.17a)

$$k = \alpha + \beta * \frac{\Delta A_i}{\sqrt{A_i}} \quad (2.17a)$$

Cross section of the excavation stretch was later introduced into the equation (2.17a) above; absolute roughness of the excavation stretch is defined by equation (2.17b)

$$k = \alpha + \beta * \frac{1}{m} * \sum_1^m \frac{\Delta A_i}{\sqrt{A_i}} \quad (2.17b)$$

α and β are constant determined experimentally and have the values of 0.15m and 0.37 respectively.

2.4.8 Solvik's method

This method is established on the measured cross section profile of the exact blasted tunnel, it describes absolute roughness k which corresponds to the local wall roughness α and effect of changes in area as absolute roughness, β . The assumption diagram used for the estimation of α and β are shown in Figures 3.1 and 3.2, respectively.

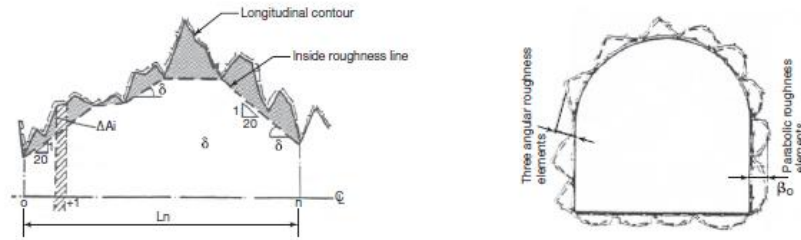


Figure 7: show α and β calculation principle sketch (Bruland & Solvik, 1987)

Solvik (1984) took 1m intervals of a profile along each wall of the tunnel and another at the top are used at to establish longitudinal sections. Straight lines are sketched along the tunnel from one extending edge to another, maintaining the slope no higher than 1:20, to create a straightened contour line (see Figure 4). The average height of the area outside the straightened contour lines is equal to α , and A is computed as follows:

$$\alpha = \frac{1}{L_n} \sum_{i=0}^n \Delta A_i \quad (2.18)$$

From figure 7, the right hand diagram shows the difference of aerial between a profile and the adjacent is converted into a group of equivalent roughness elements distributed along the perimeter. According to Bruland & Solvik (1987) value of α varies between 0.1m and 0.2m, but for a number of tunnels the mean value was found to be 0.15m.

$$\beta = 0.38 * \frac{1}{n-1} \sum_{i=0}^n \left| \frac{A_i - A_{i+1}}{\sqrt{A_i}} \right| \quad (2.19)$$

The value 0.38 is determined from measurable shapes of these roughness elements. Here, this value relates to the depth of parabolic roughness elements evenly distributed along the perimeter. For n numbers of cross-sections along the tunnel, β can be expressed as equation 2.19 and Total roughness of the tunnel, k

$$k = \alpha + 0.38 * \frac{1}{n-1} \sum_{i=0}^n \left| \frac{A_i - A_{i+1}}{\sqrt{A_i}} \right| \quad (2.20)$$

2.4.9 IBA method

Ron & Skog (1997) proposed to a new method called the “IBA method”; the method is based on a statistical treatment of wall roughness and cross section roughness by calculating *rms* (root mean square) for both. Satisfactory measurement is required in order to find the changes in data, in using this method it should be noted that it is valid when the cross section profiles are measured with narrow spacing. The wall roughness is estimated from the roughness of the three longitudinal sections measured in each tunnel section at the right wall, left wall and roof. Calculation of the wall roughness is based on *rms*, which is given by:

$$rms = \sqrt{\sum_{i=1}^n \frac{(x_i - \bar{x})^2}{n}} \quad (2.21a)$$

Furthermore, the method is based on a minimum of fifty measurements at intervals of 0.25-0.5m and the length of the longitudinal section is set to 20-25m, equivalent to 4-5 round lengths.

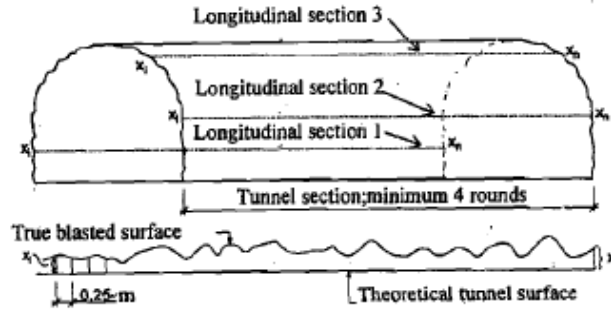


Figure 8: Principal sketch for calculating wall roughness

rms is a standard deviation and the resulting roughness is found by using variance. Resulting roughness is given by:

$$rms = \sqrt{\sum_{i=1}^m \frac{(rms_i)^2}{m}} = \sqrt{\sum_{i=1}^m \frac{VAR_i}{m}} \quad (2.21b)$$

Cross section roughness is defined as variation of cross section area. Variation of the tunnel radius can describe variation in the tunnel cross section area.

$$rms(r) = 0.53 \sqrt{\sum_{i=1}^n \frac{(A_i^{0.5} - A^2)^2}{n}} \quad (2.22a)$$

The resulting cross section roughness is calculated from the roughness found in the measured tunnel sections. The calculation is similar to resulting wall roughness:

$$rms_{wall\ cross\ section} = \sqrt{\sum_{i=1}^m \frac{(rms_i)^2}{m}} = \sqrt{\sum_{i=1}^m \frac{VAR_i}{m}} \quad (2.22b)$$

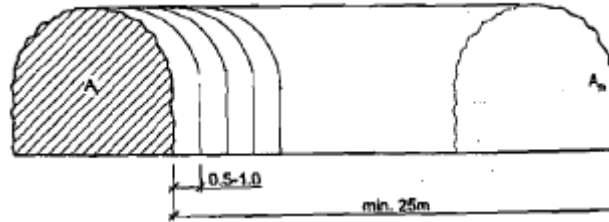


Figure 9: Principal sketch for calculating cross section roughness

Total roughness is found by adding the wall roughness and cross section roughness:

$$Total\ roughness = rms_{wall} + rms_{wall\ cross\ section}$$

A new calculation method for roughness of unlined drill and blast tunnels was proposed by Bråtveit (2015). It should be noted that the method is a theoretical suggestion and is yet to be calibrated. The method is similar to other statistical methods describe above which are based on treatment of wall and cross sectional roughness. Bråtveit (2015) method is modification of IBA method. Rather considering the variation between defined length direction and actual wall surface, the changes in distance r between the absolute cross sectional shape and the actual wall surface is estimated from small distance sections describe by dx/dy . Equation (2.21a) and (2.21b) are modified to:

$$rms_{dx,dy} = \sqrt{\sum_{i=1}^n \frac{(r_i - \bar{r})^2}{n}} \quad (2.23a)$$

Thus the total roughness is found for a chosen m of area fragments

$$rms_m = \sqrt{\sum_{i=1}^m \frac{(rms_{dx,dy})^2}{m}} \quad (2.23a)$$

In order to effectively use Bråtveit (2015) method, the analyzed tunnel sections should be a representative for the geological conditions, method of excavation and total area considering must be large enough to be statistically valid.

2.5 Existing scale model tests of unlined tunnels

The purpose of the following sections is to present a review of existing scale model tests of unlined tunnels that are available in the literature.

Andersson *et al*, (2016), investigated an experimental study of head loss over laser scan of a tunnel; the rough surface is based on a real surface that was captured by a high resolution laser scanning of a rock tunnel, a method that has been proven to be efficient for determining surface roughness. A side wall of the tunnel was extracted and scaled to 1:10 in size. The head loss inside the channel can, to an order of magnitude, was estimated and compared to a theoretical smooth channel by using the equation (2.4), the friction factor f was be evaluated by using equation (2.8a) and total roughness factor k_s is assumed to be the RMS roughness height of the surface.

	Smooth surface	Measuring section	Darcy-Weisbach
$\Delta p[\text{m}]$	0.028	0.109	0.139
$f[-]$	0.015	0.0582	0.0733

Table 5: The head loss and friction factor for the experiment (Andersson et al, 2016)

The report showed head loss increase significant comparing the first and last measured section of the channel. By assuming the RMS roughness height of the surface to be the sand grain roughness factor, the head loss could (to an order of magnitude) be estimated using the Darcy-Weisbach equation. The head loss and the friction factor in the channel is about four times higher than in a theoretical smooth channel with similar dimensions, which indicates that the rough surface has a substantial effect on the flow.

Pegram & Pennington (1996) performed a study to evaluate hydraulic roughness for the water conveyance tunnel south of Lesotho Highlands Water Project. In the investigation, measurement of tunnel roughness for concrete and shot-crete lining, and unlined sandstone and granite was achieved by a movable laser scanner; by picking up the reflection of an emitted laser beam from the tunnel wall in consecutive, discrete intervals, the wall roughness profile was digitized advancing to one particular value of the physical roughness height of the profile. Two different roughness measurements were compared against each other (standard deviation, h_σ and mean range h_λ . The physical roughness of the profile (h_σ and h_λ) obtained from the laser scanner was later equated to the

total roughness factor k_s . Using these values, friction factor f were calculated using equation (2.8a) and compared with expected values (as shown in table 6).

Method	Manning's n
(i) Colebrook-White equation (2.8a) $k_s = h_\sigma$	0.0117
(ii) Colebrook-White equation (2.8a) $k_s = h_\lambda$	0.0113
Expected value from literature	0.0100

Table 6: Estimated Manning's n values for concrete pipes (Pegram & Pennington, 1996)

They reported that using $k_s = h$ yielded results of an acceptable degree of accuracy and it could be applied with confidence of physical roughness data taken from bored tunnels, when attempting to estimate the corresponding hydraulic resistance parameters. Below are the recommended values for Manning's n for use in the design of TBM tunnels:

Cast in-situ concrete lining	$n = 0.0119 \pm 0.0009$
Unlined sandstone	$n = 0.0154 \pm 0.0010$
Unlined granite	$n = 0.0157 \pm 0.0008$
Shot-crete	$n = 0.0161 \pm 0.0011$

The conclusion of the study is that in considering the expected micro-roughness of bored tunnels, the above Manning's number n only applies to surface texture and do not incorporate macro roughness effects which is commonly encountered in TBM tunnels.

Small scale laboratory experiments of fully developed and fully pressurized turbulent pipe flow were investigated to determine the Darcy-Weisbach friction factor f by Hákonardóttir, et al., (2011). The hydraulic roughness was scaled from a 40km long unlined TBM bored headrace tunnel, the experiments include both direct measurements of pressure drop through the straight pipes and back calculations of the pressure drop from the measured roughness of the pipes. Five methods were used to estimate the measured roughness to a hydraulic roughness coefficient. Two of the methods used in the study were from Pegram & Pennington (1996), here equivalent physical roughness of the profile h_σ was taken as twice the amplitude, a , of the equivalent sinusoid fitted through a roughness profile. The five methods are given below:

- (i) Heerman's empirical equation (2.8c)
- (ii) Colebrook-White equation (2.8a) $k_s = h_\sigma$
- (iii) Colebrook-White equation (2.8a) $k_s = h_\lambda$
- (iv) Colebrook-White equation (2.8a) $k_s = 2h_\sigma$
- (v) Colebrook-White equation (2.8a) $k_s = 2h_\lambda$

It was suggested that amplitude depends only on the standard deviation roughness profile, but not on the wave length of the sinusoid and is given by:

$$h_\sigma = 2a = 2(2\sigma)^{0.5} \quad (2.24a)$$

$$h_\lambda = \frac{1}{T-\lambda} \sum_{i=1}^{T-\lambda} r_i \quad (2.24b)$$

The test results indicated the methods (i)–(v) could be used for estimating hydraulic roughness for a measured roughness profile, also stated that any methods to be used in calculating hydraulic roughness depends on some factors characteristics of roughness and height scale of the roughness elements is more important than the spacing between the relative depth between the elements.

CHAPTER THREE

3.0 EXPERIMENTAL SETUP

3.1 Unlined tunnel model set up

The setup of the unlined tunnel determines how the roughness is created in this study. The appropriate use of the available apparatus and the individual limitations of each item of equipment is what will limit the overall accuracy of the results obtained.

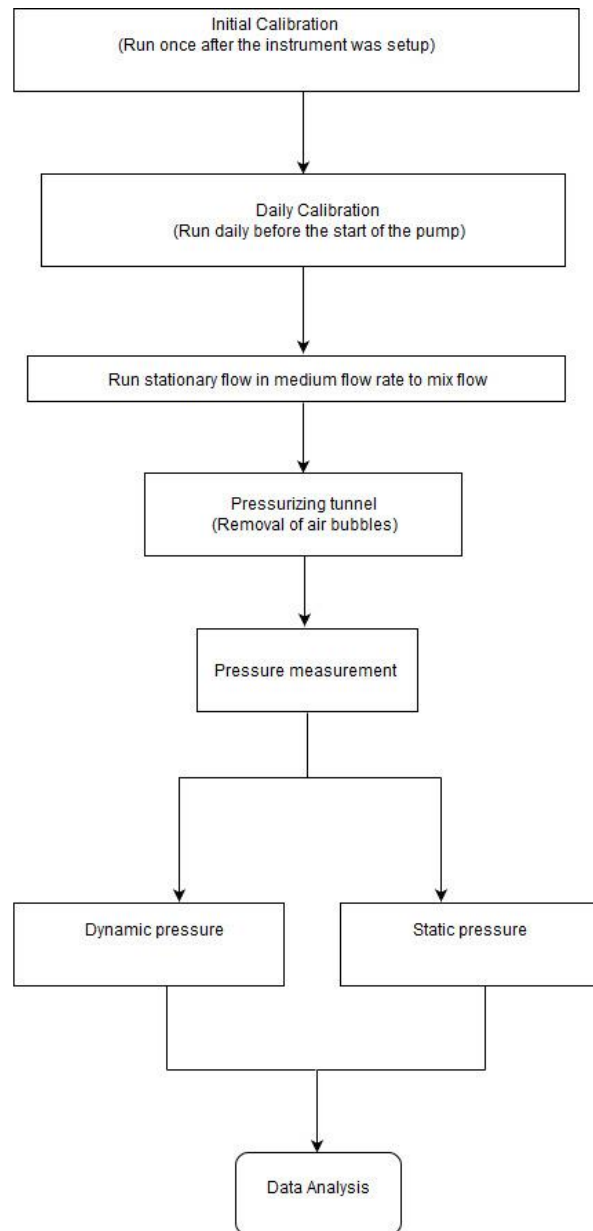


Figure 10: Measuring procedures

The experiments were carried out at the NTNU hydropower laboratory; the tests were carried on two tunnel models (Tunnel A & B), which are made up of Plexiglas channel having rough sidewalls. The

rough surface in Tunnel A and Tunnel B (figure 11a & 11b) is created by strips is 0.015m thick, has a length of 0.60m with an average spacing of 50mm and 0.005m thick, length of 0.425 and average spacing 1m respectively. Tunnel A is 5.85 m long to allow the flow to be developed, having a slope 0.02 from the upstream to the downstream of the tunnel which provides stable driving flow and a mesh is placed at the entrance of the tunnel to straighten the flow.



Figure 11a: Tunnel A

Figure 11b: Tunnel B

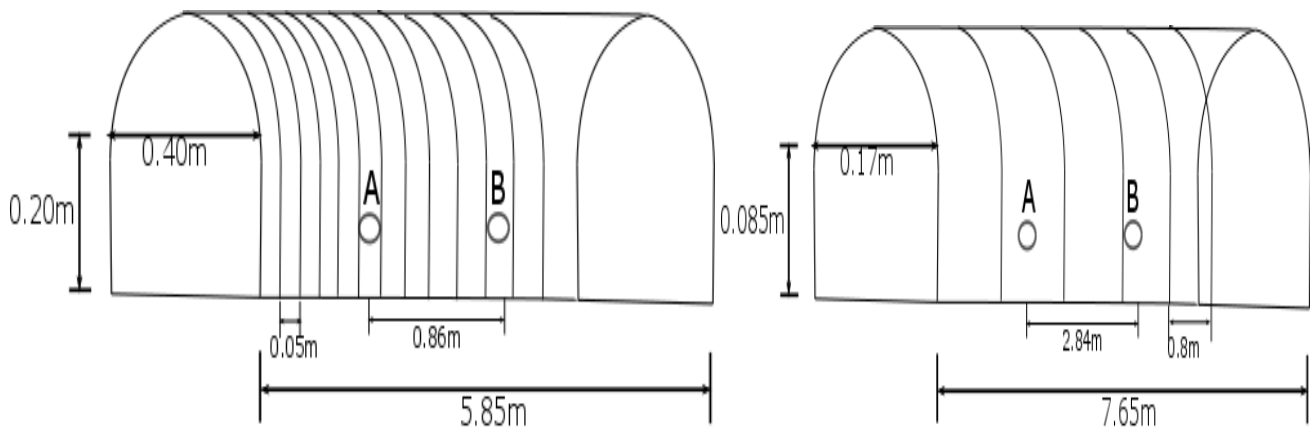


Figure 12: schematic diagram of tunnel A & B showing cross-sections and strips spacing
 The flow through the channel is pressure driven; the head is adjusted by regulating the water level in the column placed before the channel outlet (Figure 11), and the water level is regulated by a valve placed at the extreme end of the tunnel. The flow rate was regulated by adjusting the inlet valve and flow meter for visual are connected to the loop; 100 liters pump was controlled by a PID-regulator, which supplies water to the system. Several flow rates were used in the tests which will be discussed in subsequent sub-sections and differed about $\pm 3\%$ throughout the measured sets.

3.1 Calibration of pressure sensor

The Aplisen differential pressure sensor (APR-2000ALW) measures the difference in pressure $P_{s_a} - P_{s_b} = \Delta P$ and displays this in mH₂O. The calibration of the pressure sensor was achieved by connecting the pressure tube of the instrument to a digital gauge, the pressure tubes were set at the same height, keeping one of tube fixed. Exactly 10 minutes after setting up the instrument, the actual reading started and at every 5 minutes interval the height is increased to 10mm was done till 80mm. Calibration of the pressure sensor was nominally done once a day before actual measurement is taken, the observed pressure head from the tube connected to the sensor has a linear relationship to the mH₂O display, thus best fit line describes the response of the pressure sensor allowing any correction to be measured into actual pressure reading. Daily calibration was conducted when the water was still, normally before the first start-up of the pumps. Usually the relation between a pressure transmitter input and output is predominantly linear ($Y = ax + b$), where a is known as gain and b is zero or offset and function of the measured values during calibration.

- Zero reset of differential sensors
- Zero reset of Aplisen Raport 2 software
- Zero reset of flow rate meter

The above calibrations were carried out from both positive and negatives tubes of the differential pressure sensor and Aplisen remote software at the same time, sometimes there was air encompassed and accumulated at the top of the tunnel, it was released before the daily calibration.

3.2 Dynamic pressure

The difference between the total pressure and the appropriate static pressure is directly related to the dynamic pressure at that position. Experimental set up for measuring dynamic pressure was done by connecting the pitot tubes to the tunnel such that both pitot tubes are perpendicular to the flow.

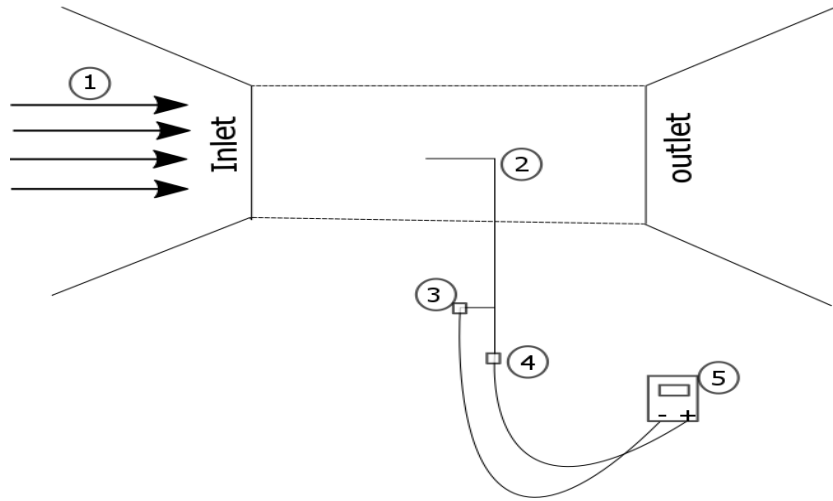


Figure 13: schematic diagram of dynamic pressure measurement (1) Flow direction (2) Pitot tube (3) Static pressure tap (4) Total pressure tap (5) Differential pressure sensor

Total pressure tap is connected to the high pressure port and static pressure is connected to the low pressure port of the Aplisens differential pressure sensor respectively. Dynamic pressures for both points were measured with different discharges.

3.3 Velocity profile

The velocity profile was calculated from the dynamic pressure measurements, velocity at each pitot measurement location can be calculated using Bernoulli relation. At pitot measurement location down the tube, the velocity at a measurement location can be derived from the difference in total and static pressures

$$u = \sqrt{2 \frac{p_t - p_s}{\rho_{water}}} \quad (3.1)$$

The pitot tubes were placed at different width of the tunnel and this was done for the both measuring points (i.e. measuring point A and point B) and it should be noted that velocity profiles that were been reduced are not planar but rather axisymmetric in nature. The proper way to calculate average velocity is to integrate over and then divide by width of the tunnel.

$$\bar{u} = \frac{1}{w} \int_0^w u(y) dy \quad (3.1a)$$

3.3 Pressure drop or Headloss

Recall that hydraulic loss is equal to the head of pressure drop or head loss, the pressure measured by the instrument is static differential pressure with respect to the fluid. The pitot tubes were placed on two points in between the roughness of the tunnel. The Pitot tube was inserted into the tunnel with the tip pointed toward the flow of the water. The negative port of the differential pressure sensor is connected to the static pressure port of the pitot at point A and the positive port of differential pressure sensor to the static pressure port of the pitot at point B. The differential pressure sensor then displayed differential pressure, both pitot tubes measures the difference in pressure between two points located close to the wall in the inlet and outlet of the tunnel, all measurements ran between 40-50 minutes and were repeated 3-4 times.

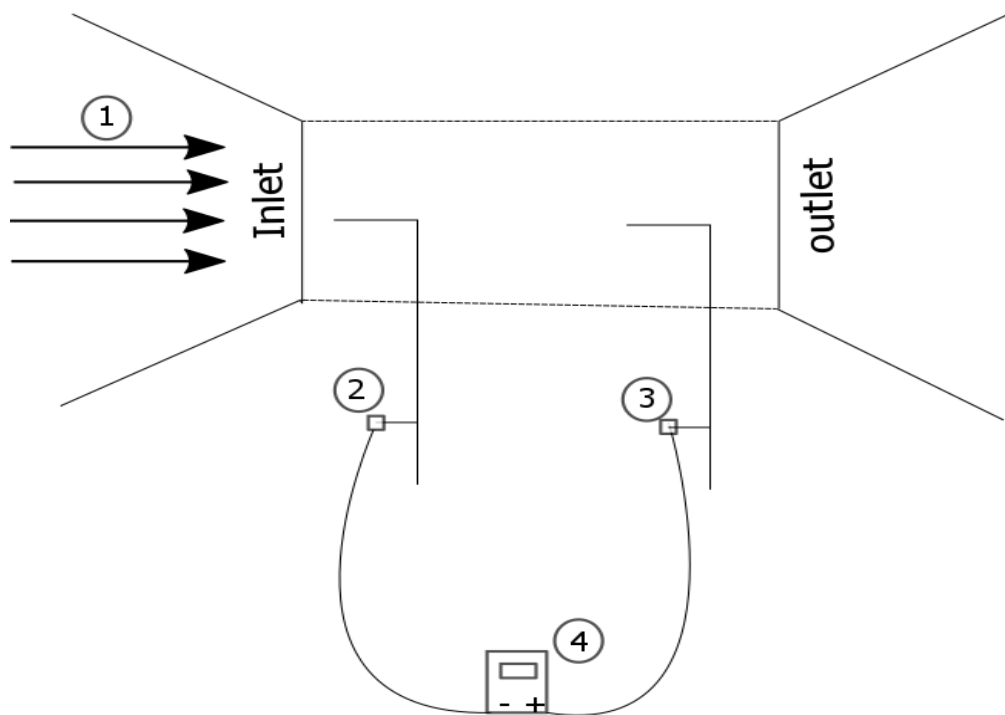


Figure 14: schematic diagram of differential static pressure measurement (1) Flow direction (2) & (3) Static pressure tap (4) Differential pressure sensor

CHAPTER FOUR

4.0 RESULTS AND DISCUSSION

4.1 Calibration of Differential Pressure Sensor

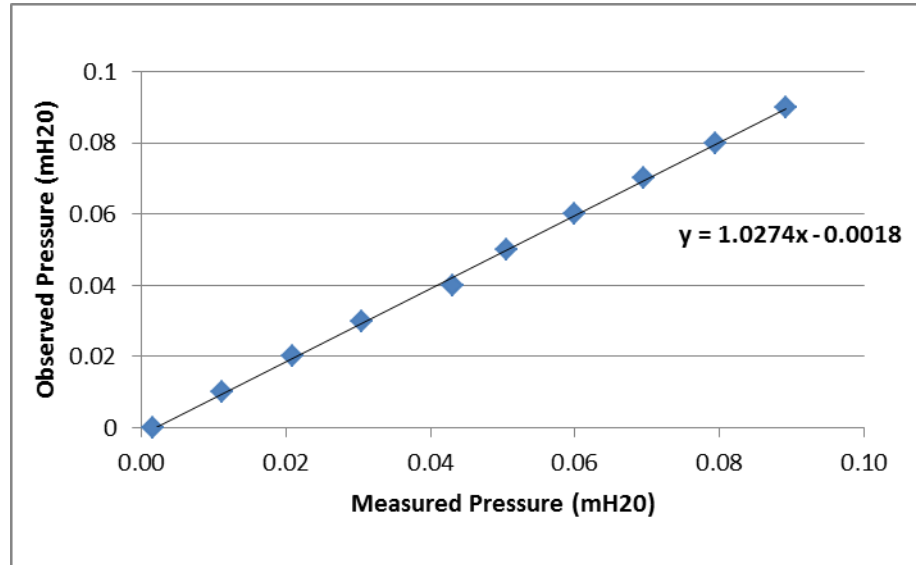


Figure 15: Linearization of observed measurement against instrument measurement

The error due to calibration is due to the error associated with the pressure measurement by the sensor. A resolution of 0.01 mH2O corresponds to an error of 0.1% at the operating flow rate of this experiment. This error would however be significant at lower velocities. The coefficients obtained were used to linearize the outputs of the sensor over the transmitter's entire pressure measurements reading and the uncertainty of estimating the true static differential pressure is reduced.

4.2 Dynamic pressure

In Figure 16, the measurements of dynamic pressure by using the pitot tubes placed on the center width of the tunnel are visualized along with each pressure time series. The highest mean dynamic pressures can be found in measuring point A, which is located in close to inlet of the tunnel. The high pressure in these zones indicates that increase in velocity in that area due to closeness between inlet valve and measuring point A, which is to be expected.

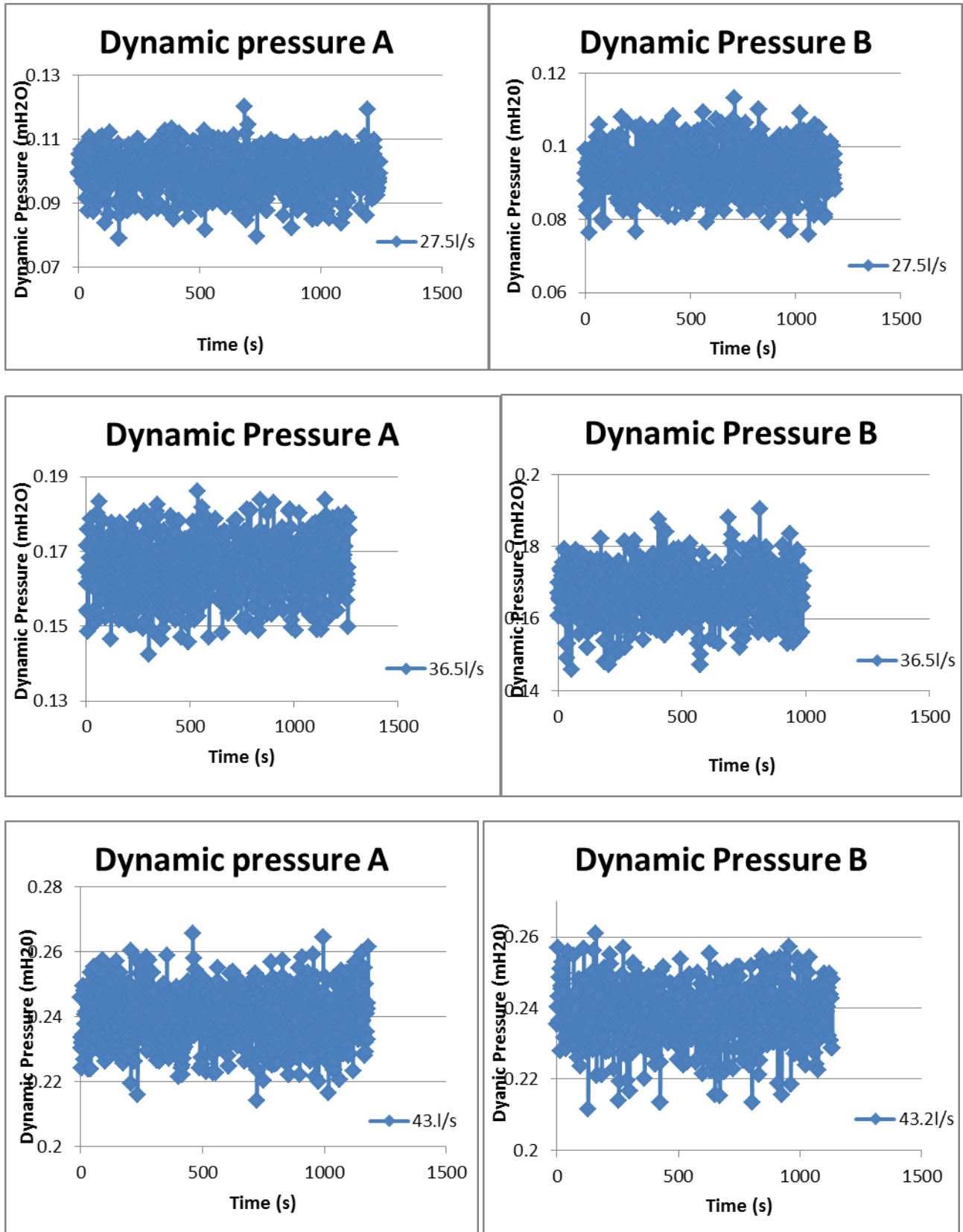


Figure 16: Dynamic pressure plotted against time for different charges (Tunnel B)

4.3 Velocity profile

Generally the data is non-linear (somewhat parabolic), with the maximum velocity occurring near the centerline of the tunnel and the minimum occurring near the wall. In fact, the maximum velocity was seen between 11cm to 13cm of the tunnel, from the centerline, although the variation of velocity in that region is close to the calculated velocity. The fact that the velocity drops off near the wall makes sense, since the velocity is decreasing at the wall because of the no-slip condition. The shape of the velocity profile suggests that the flow is turbulent. First, the velocity profiles are somewhat parabolic, but nearly curve from the centerline of the tunnel to about two inches away. Second, the velocity decreases sharply near the wall. Both of these features are characteristic of turbulent flow.

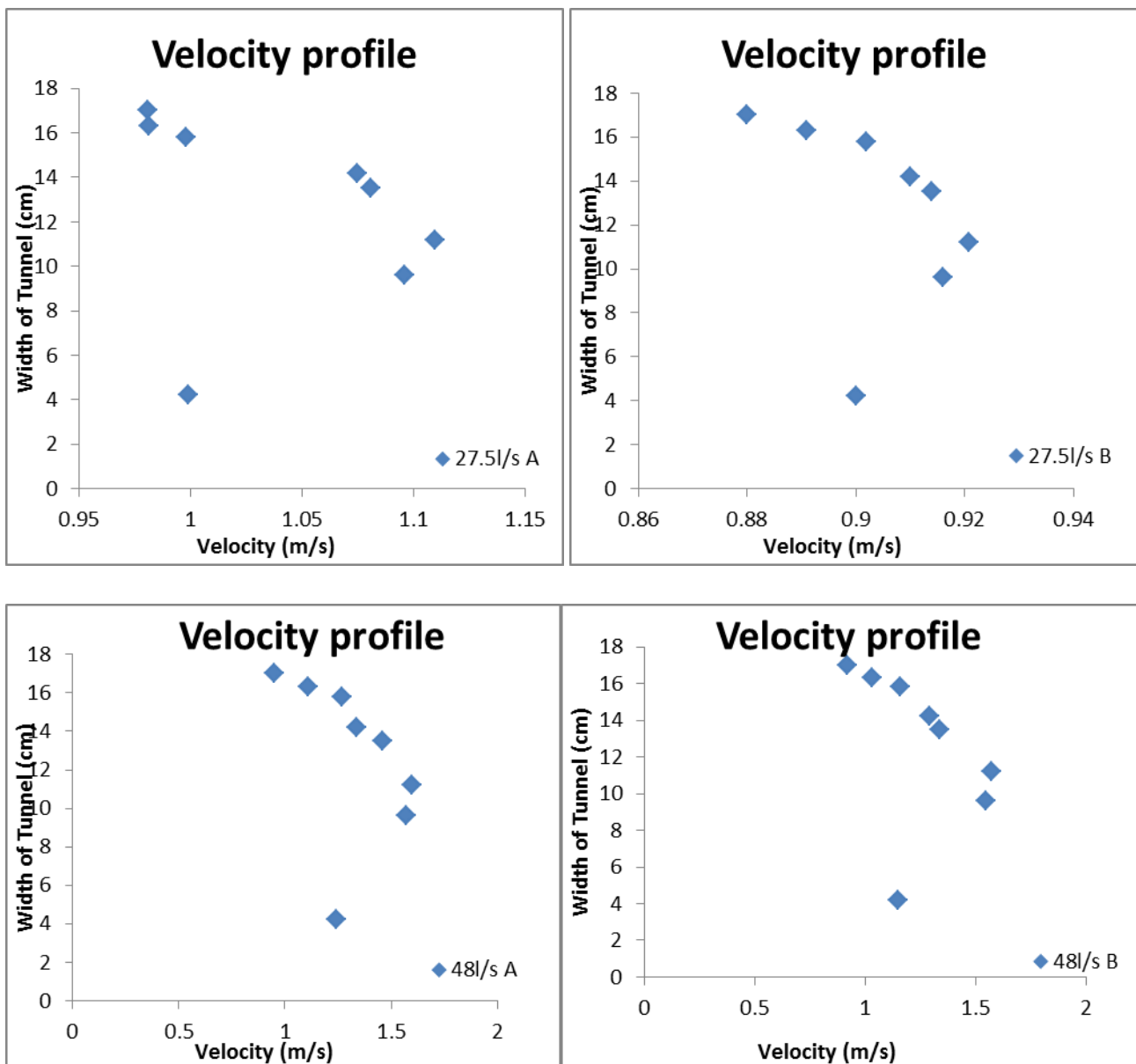


Figure 17: depicts the measured velocity as a function of position in the Tunnel B

Finally, the fluctuations in differential pressure sensor readings could be due to turbulence, although fluctuations will occur in any flow, laminar or turbulent. Because the pressurized flow is driven by closing the outlet valve, it is possible that the vibration inside and outside tunnel, or swirling, despite the presence of the mesh in the tunnel.

4.4 Pressure Drop and Headloss

The variation of pressure measurements with the streamwise distance has a similar trend for all tests. In general, the static pressure measurement was nearly constant for all reading taken except little drop and increase in values, mostly occurred all discharges (Figure 17), the variation could be associated with the sensitive of the instrument. The results from dynamic pressure and velocity profile made it possible where to place the pitot tubes, results below is taken from 11 cm-13cm width of the tunnel.

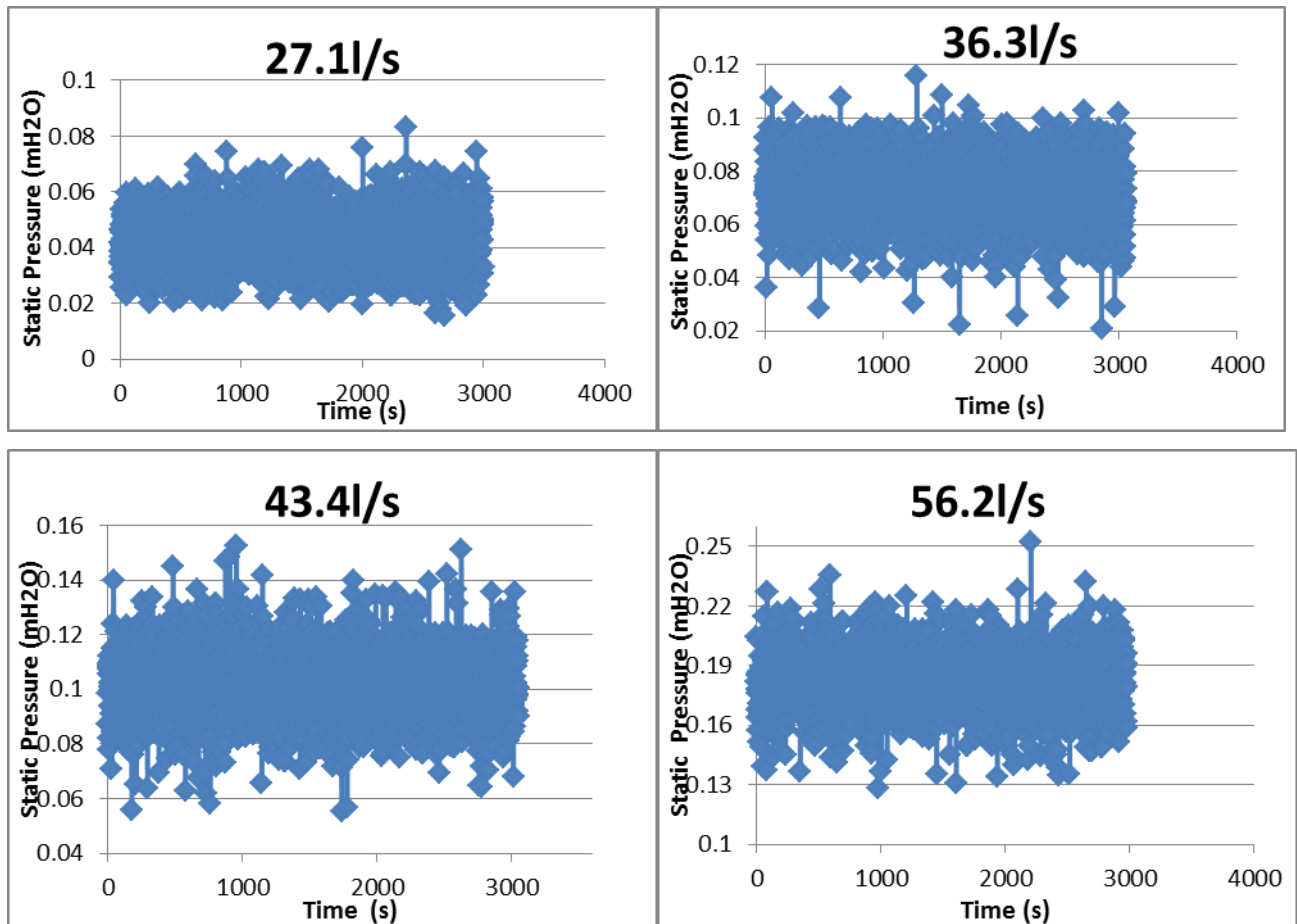


Figure 18: measured static differential pressure as a function of time (Tunnel B)

The pressure drop across the tunnel increases with the increase in discharge. The preceding discussion indeed shows that the dynamic pressure are proportional to head loss in the Tunnel B, resulting in an almost constant number for the ratio of head loss and dynamic pressure head,

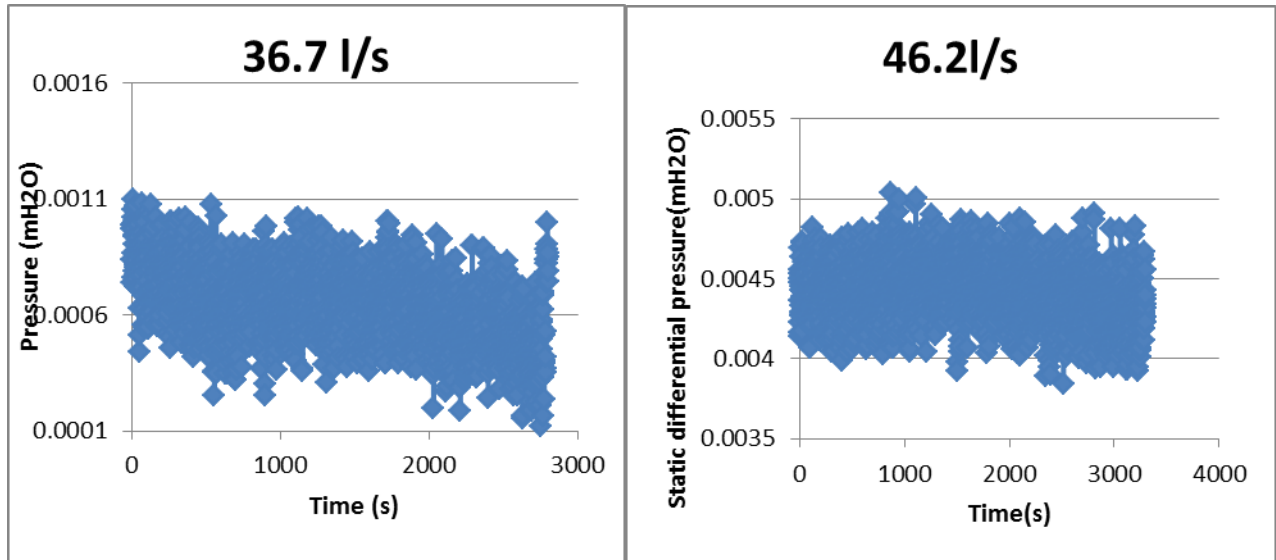


Figure 19: measured static differential pressure as a function of time (Tunnel A)

Unlike study of Andersson, *et. al* (2016) where the differential pressure was increasing throughout the channel Figure 19 shows discharge (Q) versus the mean value of differential static pressure(p) for various test conducted.

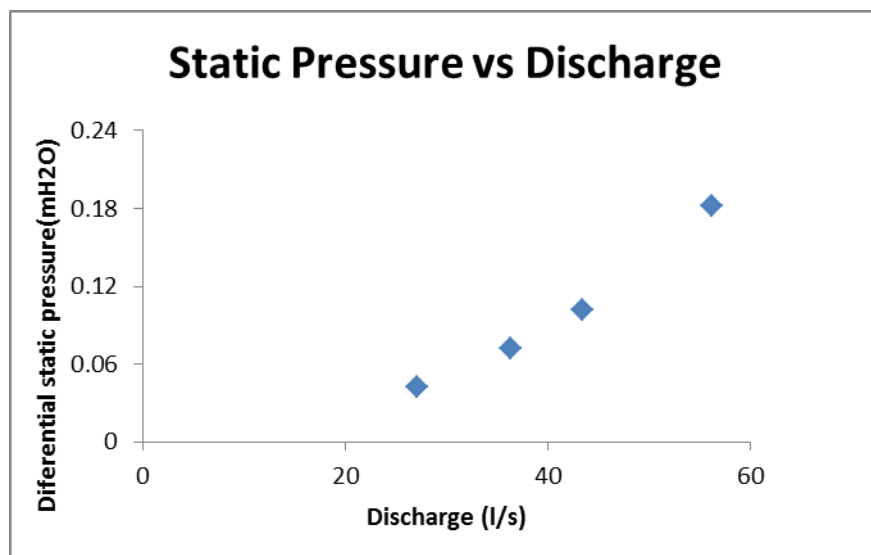


Figure 20: Static pressure plotted against discharge

4.5 Comparison of roughness in both tunnels

Frictional factor and relative roughness are one of the factors which need to be known in designing hydropower tunnels, this was estimated for both tunnel using Darcy-Weisbach equation (Equation 2.4), Colebrook-White formula (Equation 2.8b), knowing the diameter, flow rate and head loss along tunnel stretch of length L. Comparison between friction factor measured for Tunnel A and Tunnel B was made. The results are presented below:

Q (m³/s)	h_f (m)	f (-)	K_s/D
0.0367	0.0006	0.083	0.063
0.0462	0.0043	0.104	0.097

Table 7: Average headloss, frictional factor and Relative roughness for Tunnel A

Q (m³/s)	h_f (m)	f (-)	K_s/D
0.0363	0.072	0.03	0.004
0.0433	0.102	0.03	0.004
0.0562	0.182	0.05	0.021

Table 8: Average headloss, frictional factor and Relative roughness for Tunnel B

Comparing the both wells in this study, it was found that Tunnel A is rougher than Tunnel B (Table 7 & 8), it was expected as seen one figure 11 & 12, the strips spacing, thickness and height could be the reason Tunnel A yielded higher friction factor values. The effect of these factors on roughness characteristics have dominant on headloss to boundary roughness in both tunnels, which is in agreement with Pennington (1998) report that the number of head loss depends on size of eddy generated which is directly proportional on the roughness projection that the eddy is spawned and the frequency of eddy generation is dependent on the spacing between consecutive roughness projections. The similarity between these values obtained from the laboratory measurements and those found in the literature is encouraging.

CHAPTER FIVE

5.0 CONCLUSION

This study has proven the importance scale model of tunnels in order to relate the experimental result of frictional and energy losses to the physical structure of tunnel roughness. Several pressure measurements of flow over a rough surface were performed in two different tunnels at different discharges. The study revealed a range of dynamic pressures and static differential pressure depending on the spacing and height of roughness element, high dynamic pressure in measuring point A (Tunnel B) indicates that increase in velocity in that area due to closeness between inlet valve and measuring point, furthermore dynamic pressures of different position in the tunnel which was later converted to velocity, the velocity decreases near the wall. The shape (parabolic) of the velocity profile suggests that the flow is turbulent. The differential pressure measurements showed a significant increase of head loss comparing Tunnel A and Tunnel B in the whole experimental campaign.

Comparison between the friction factors and relative roughness of both tunnels calculated with the Darcy-Weisbach and Colebrook-White equation led to the conclusion that the head loss depends on size of eddy generated which is directly proportional on the roughness projection that the eddy is spawned and the frequency of eddy generation is dependent on the spacing between consecutive roughness projections.

REFERENCES

- Aberle, J., Henry, P.-Y., Bråtveit, K. (2017). Linking physical wall roughness of unlined tunnels to hydraulic resistance – The Tunnel Roughness project. Proceedings of the World Tunnel Congress 2017 – Surface challenges – Underground solutions. Bergen, Norway.
- Arngrímsson, H.Ö. & Gunnarsson, Þ. B. (2009). Tunneling in acidic, altered and sedimentary rock in Iceland. Master thesis, Technical university of Denmark. Retrieved from [http://www.vegagerdin.is/vefur2.nsf/Files/Tunneling_Budarahalsvirkjun_MSc_Ritg/\\$file/Tunneling_Budarahalsvirkjun_MSc_Ritg.pdf](http://www.vegagerdin.is/vefur2.nsf/Files/Tunneling_Budarahalsvirkjun_MSc_Ritg/$file/Tunneling_Budarahalsvirkjun_MSc_Ritg.pdf)
- Andersson, L., Larsson, I., Hellstrom, J., Andreasson, P., Andersson, A. (2016). Experimental Study of Head Loss over Laser scanned Rock Tunnel. In B. Crookston & B. Tullis (Eds.), Hydraulic Structures and Water System Management. 6th IAHR International Symposium on Hydraulic Structures, Portland, OR, 27-30 June (pp. 22-29). doi:10.15142/T360628160853 (ISBN 978-1-884575-75-4).
- Benson R. P. Design of unlined and lined pressure tunnels. In Canadian Tunnelling 1987/88, Bitech, Vancouver (1989).
- Bråtveit, K. (2015), Effects of load fluctuation on hydropower tunnels. Thesis submitted in partial fulfillment of requirements for PhD, Department of Hydraulic and Environmental Engineering, Norwegian University of Science and Technology.
- Bråtveit, K. and Olsen, N. R. B. (2015), Calibration of horizontal acoustic doppler current profilers by three dimensional CFD simulations (OpenAccess), Engineering Applications of Computational Fluid Mechanics, Vol. 9, Issue 1, pp 41-49.
- Bishwakarma, M. B. (2012), Computation of Head Losses in Hydropower Tunnels. Retrieved from https://www.researchgate.net/publication/280609552_Computation_of_Head_Losses_in_Hydropower_Tunnels?ev=prf_high
- Broch, E., (2013), Underground hydropower projects, - lessons learned in home country and from projects worldwide. I: Norwegian hydropower tunnelling II. : Norwegian tunnelling society 2013 ISBN 978-82-92641-28-6. s. 11-19 NTNU
- Broch, E., (2000), Unlined high pressure tunnels and air cushion surge chambers. I: Tunnels under Pressure. AITES-ITA 2000 World Tunnel congress. Johannesburg: The South African Institute of Mining and Metallurgy 2000 ISBN 1-9197831-1-3. s. 63-72 NTNU
- Broch, E., (1982), Designing and excavating underground powerplants, Water Power and Dam Construction 34:4, 19-25.

- Broch, E., (1982B), The development of unlined pressure shafts and tunnels in Norway. *Rock Mechanics: Caverns and Pressure shafts* (Wittke, Ed.), 545-554. A.A. Balkema, Rotterdam, Netherlands. Also in *Underground space* No.3 1984
- Bruland, A & Sohkrollah, Z. (2001), Comparison of tunnel blast design models *Tunneling and underground space technology* 21,
- Bruland, A., Solvik, Ø., 1987. Analysis of roughness in unlined tunnels. In: *Proceedings of the International Conference (Underground Hydropower Plants)*, Oslo, June 22–25, pp. 701–709
- Colebrook, C.F., (1939), Turbulent flow in pipes with particular reference to the Transition Region between the Smooth and Rough Pipe Laws, *Journal Inst. of Civil Engrs.*, 11, pp 133-156.
- Colebrook, C.F., (1958), The flow of water in unlined, lined, and partly lined rock tunnels. *Journal Inst. of Civil Engrs.*, E-ISSN 1753-7789, Volume 11 Issue 1, SEPTEMBER 1958, pp. 103-132
- Deere, D.U., (1983), Unique geotechnical problems at some hydroelectric projects. In *Seventh Pan Am Proc.*, Vancouver, pp. 865-88. Canadian Geotechnical Society.
- Elger, D.F., Crowe, C.T., Williams, B.C., & Roberson, J.A. (2010), *Engineering fluid mechanics* (9th edition). Hoboken: John Wiley & Sons, Inc
- Eydísardóttir, A.H., (2013), Relating measured physical roughness of hydropower waterways to hydraulic roughness, M.Sc. thesis, Faculty of Civil and Environmental Engineering, University of Iceland
- Fischer, J. A., Garcia, G., Pennington, T. W., & Richards, D. P. (2009). A review of tunneling difficulties in carbonate sedimentary rocks. 2009 Rapid excavation and Tunneling Conference Proceedings (ss. 215-230). Colorado: Society for Mining, Metallurgy, and Exploration, Inc.
- Flack, K.A., and Schultz, M.P., (2014) Roughness effects on wall-bounded turbulent flows Department of Mechanical Engineering, United States Naval Academy, Annapolis, Maryland 21402, USA. Department of Naval Architecture and Ocean Engineering, United States Naval Academy, Annapolis, Maryland 21402, USA *PHYSICS OF FLUIDS* 26, 101305.
- George, A.M., (2016), The World Bank. [ONLINE] Available at: <http://www.worldbank.org/en/news/feature/2016/02/17/africa-far-from-sustainable-energy-for-all-but-showing-signs-of-progress>.
- Hákonardóttir, K.M., Pálmason, P.R., Kasprzyk, A. & Filipek, K. (2011). Converting wall roughness to hydraulic roughness in fully turbulent pipe flow: Small-scale experiments and large-scale measurements at the Kárahnjúkar HEP, Iceland. Retrieved from http://www.verkis.is/media/frodleikur/2011-hydro-hakonardottir_paper.pdf

- Hákonardóttir, K.M., Tómasson, G.G., Kaelin, J., and Stefánsson, B. (2009). The hydraulic roughness of unlined and shotcreted TBM-bored tunnels in volcanic rock: In situ observations and measurements at Kárahnjúkar Iceland”. *Tunnelling and underground space technology* 24(6), pp. 706–715.
- Heerman, D.F., (1968), Characterization of hydraulic roughness, Thesis submitted in partial fulfillment of requirements for PhD, Colorado State University, Colorado.
- Hudson, J.A., (1992), *Rock Engineering Systems: Theory and Practice*, Horwood, Chichester, 185 pages
- Huval, C.J. (1969) "Hydraulic Design of Unlined Rock Tunnels" *Journal of Hydraulics Division, American Society of Civil Engineers*, Vol 95, No. HY4, Proc Paper 6679, pp 1235-1246.
- Koh, Y., (1992) Turbulent flow near a rough wall," *J. Fluids Eng.*, Vol. 114, pp. 537-542.
- Lahiouel, Y., & Lahiouel, K., (2015), Evaluation of Energy Losses in Pipes. *American Journal of Mechanical Engineering*, vol. 3, no. 3A (2015): 32-37. doi: 10.12691/ajme-3-3A-6.
- Moody, L.F., (1944), “Friction Factors for Pipe Flow”, *Trans. American Society of Mechanical Engineers.*, 66, pp 671-684.
- Müller, L., 1978. *The Rock Engineering. Third Volume: Tunneling*, Salzburg, Ferdinand Enke Verlag, Stuttgart, (In German).
- Nikuradse, J., (1933), “Strmungsgesetze in Rauben Rohren”, *Verein Deutscher Ingenieure, Forschungsheft*, p 361.
- Nilsen B & Palmstrøm A (2000): “Engineering Geology and Rock Engineering”. NBG (Norwegian Group for Rock Mechanics), Handbook No.2, 249 p.
- Norwegian Ministry of Petroleum and Energy (2008), *Facts report on Energy and Water resources in Norway*. 07 Oslo, 2008 ISSN 0809-9472.
- Palmström A., (1987): Norwegian design and construction experience of unlined pressure shafts and tunnels. *International Conference on Hydropower*, Oslo, Norway, 1987.
- Panthi, K.K., & Basnet, C., (2016), Review on the Major Failure Cases of Unlined Pressure Shafts/Tunnels of Norwegian Hydropower Projects. *Hydro Nepal Journal of Water Energy and Environment*. DOI: 10.3126/hn.v18i0.14637
- Pennington, M.S., (1998), Hydraulic roughness of bored tunnels. *IPENZ Transactions*, Vol. 24, No. 1/CE.

Pegram, G.G.S. & Pennington, M.S., (1996), A method for estimating the hydraulic roughness of unlined bored tunnels”, Report to the Water Research Commission by the Department of Civil Engineering, University of Natal, WRC Report No 579/1/96. ISBN No. 1 86845 219 0.

Priha, S., (1969), Hydraulic properties of small unlined rock tunnels. Journal of the Hydraulics Division, 95(4):1181–1210.

Powe, R. E. and Townes, H. W., (1973), Turbulence structure for fully developed flow in rough pipes," J. Fluids Eng., pp. 255-261.

Rahm, L. (1958), Friction losses in Swedish rock tunnels. Water Power, December., pp. 457-464.

Reinius, E., (1970), Head losses in unlined rock tunnels. Water Power July / August

Rønn, P E & Skog, M, (1997), New Method for Estimation of Head Loss in Unlined Water Tunnels’, Proceedings, International Conference on Hydropower, Trondheim, Norway.

Salazar, G.F., (1985), Simulation Model for Tunneling Through Difficult Ground Conditions. Department of Civil Engineering, Worcester Polytechnic Institute, Worcester, Massachusetts.

Solvic, Ø, (1984) “Roughness and Roughness Analysis of Unlined Blasted and TBM Tunnels in Norway”, Proceedings, International Symposium: Tunnelling for Water Resource & Power Projects, New Delhi, India.

Tarkoy, P. J., (1995), Comparing TBMs with drill & blast excavation. Tunnels & Tunneling, October, 41–44.

Webb, R.L., Eckert, E.R.G. & Goldstein, R.J., Heat transfer and friction in tubes with repeated-rib roughness," Int. J. Heat Mass Transfer, Vol. 14, pp. 601{617, 1971.

White, F. M. (2009). Fluid mechanics (6th edition). New York: McGraw-Hill

World Energy Resources, WER (2016), Report on Hydropower consumption, https://www.worldenergy.org/wp-content/uploads/2017/03/WERResources_Hydropower_2016.pdf accessed February, 03 2017